Matr. N 15935

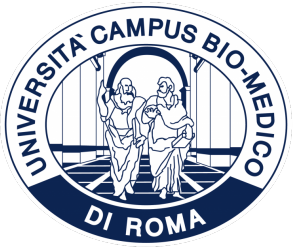

UNIVERSITÀ CAMPUS BIO-MEDICO DI ROMA

Facoltà Dipartimentale di Ingegneria

Corso di Laurea in Ingegneria Industriale

STRUCTURAL IDENTIFICATION OF OIL SUPPLY, GLOBAL DEMAND AND SHOCKS: A FACTOR ANALYSIS WITH INDUSTRIAL APPLICATIONS

Relatore

Ch.mo Dott. Marco Papi

Laureando

Gianluca Adriano Junior Addorisio

ANNO ACCADEMICO 2024/2025

To my parents

Sommario

Questa tesi analizza i meccanismi strutturali che guidano le oscillazioni del prezzo del petrolio e ne valuta le implicazioni per la gestione del rischio carburante nel settore del trasporto aereo. Viene costruito un dataset mensile 1990–2024 su produzione USA, attività economica OCSE, scorte petrolifere USA e prezzo reale del WTI, viene stimato un modello VAR a quattro variabili su trasformazioni stazionarie, evidenziando l'inadeguatezza delle regressioni statiche e la necessità di un approccio dinamico multivariato.

Lo SVAR è identificato mediante restrizioni di segno in stile Kilian–Murphy, distinguendo shock di offerta, shock di domanda aggregata e shock precauzionali. Gli shock estratti presentano deviazioni marcate dalla normalità e forte dipendenza di coda, confermata tramite copule t. Le risposte agli impulsi mostrano che la domanda globale è il principale driver del prezzo del WTI nel medio periodo, mentre gli shock di offerta sono poco persistenti e quelli precauzionali diventano rilevanti soprattutto negli eventi estremi.

Questi risultati alimentano la generazione di scenari di prezzo e un esercizio di stress test ispirato a una chiusura dello Stretto di Hormuz. La mappatura verso il prezzo del Jet Fuel e l'applicazione al caso ITA Airways indicano che una copertura lineare completa riduce sensibilmente l'esposizione ai picchi di prezzo determinati da shock di offerta estremi.

Abstract

This thesis investigates the structural drivers of crude oil price fluctuations and their implications for fuel-price risk management in energy-intensive industries. Using monthly data for 1990–2024, a four-variable VAR is estimated on stationary transformations of world oil production, OECD real activity, petroleum inventories and the real WTI price. Reduced-form evidence shows that static regressions are unstable and severely misspecified, motivating a dynamic multivariate approach. A structural VAR is then identified through sign restrictions in the spirit of Kilian and Murphy (2014), disentangling flow-supply, aggregate-demand and precautionary shocks. The structural shocks exhibit marked non-Gaussian features, strong leptokurtosis in demand and precautionary innovations, and significant tail dependence, captured through t-copulas. The estimated impulse responses imply that global demand is the dominant source of medium-run WTI variability, while supply shocks are short-lived and precautionary shocks contribute primarily through extreme events. These results feed into model-based scenario generation and a stress test calibrated on a Strait of Hormuz-type disruption. Mapping WTI paths into jet fuel prices, and applying them to the fuel bill of ITA Airways, shows that a full linear hedge substantially attenuates the cost impact of extreme supply disruptions.

Contents

List of Figures

List of Tables

Chapter 1

Introduction

1.1 Motivation and Background

Understanding the behaviour of crude oil prices is critical for macroeconomic analysis, financial stability and industrial decision-making. Oil remains the world's most strategic commodity, influencing inflation, business cycles, transportation networks and geopolitical dynamics. Because crude oil serves both as a physical input and as a financial asset, its price reflects a complex interaction between real fundamentals, expectations, inventories, speculative pressures and policy events. As argued by Barsky and Kilian [3, 4], macroeconomic outcomes associated with oil price movements cannot be understood through a simplistic focus on physical supply disruptions alone.

A central insight of the modern literature is that oil price fluctuations predominantly reflect global aggregate demand conditions and changes in precautionary inventories rather than supply-side disturbances. In the structural decomposition of Kilian [14], shocks to global real economic activity account for the majority of medium-run oil price variation, while precautionary demand shocks — captured through inventory dynamics — generate sharp price spikes during episodes of uncertainty about future availability. More recent contributions [15, 5] confirm these findings and refine the understanding of speculative motives and inventory behaviour.

Despite substantial progress in modelling, a persistent misconception in public and policy discussions is that oil price spikes are mainly supply-driven. Structural evidence, however, contradicts this view: most large post-1990 price surges were demand-led rather than the result of physical shortages[17]. Historical accounts further reinforce this interpretation, showing that many so-called "supply crises" were in fact driven by shifts in global demand, precautionary behaviour, or broader macroeconomic conditions[8]. However, the empirical evidence overwhelmingly shows that supply shocks are relatively rare, generally small in magnitude and have limited persistence. The short-run price elasticity of crude oil supply is extremely low, reflecting physical and technological constraints in the extraction sector. Consequently, even small shifts in global economic activity or revisions in expectations can produce outsized price movements.

The complexity of the oil market extends beyond macroeconomic theory. For industries that rely heavily on refined petroleum products — particularly aviation — fluctuations in oil and jet fuel prices translate into substantial financial risk. Fuel expenses typically represent between 20% and 35% of airline operating costs [11]. This exposure makes airlines highly vulnerable to extreme price movements arising from macroeconomic or geopolitical shocks. For this reason, the aviation sector requires robust risk management tools capable of mapping crude oil disturbances into jet fuel prices and quantifying the impact on cash-flow and budgeting decisions.

Modern risk management increasingly relies on scenario-based methods that integrate economic fundamentals. Firms can no longer depend on simple forecasting tools or static projections, as such models fail to capture the structural origins of volatility. Instead, firms look towards econometric frameworks capable of isolating the underlying drivers of price movements and generating both probabilistic scenarios and adversarial stress tests [1, 26]. Structural VAR (SVAR) models, in particular, offer a theoretically grounded method for disentangling supply, demand and inventory shocks, while copula-based approaches allow researchers to characterise nonlinear dependence and tail-risk interactions across shocks.

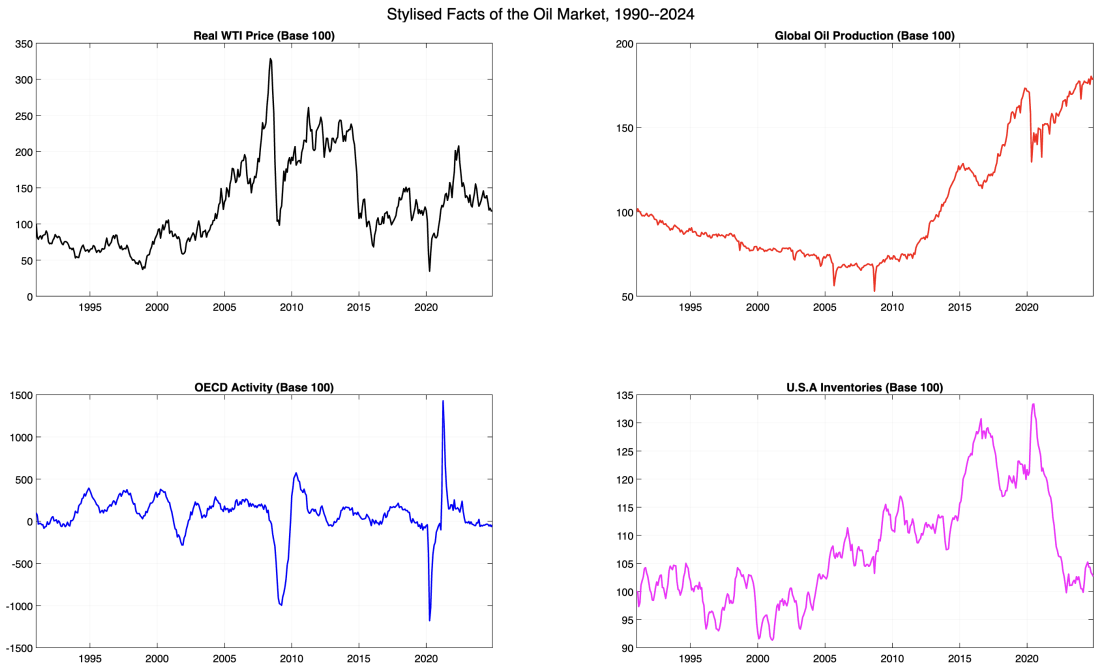

Figure 1.1: Stylised Facts of the Oil Market, 1990–2024: Real WTI Price, OECD Activity, Oil Production, Oil Inventories. (*Source*: own elaboration on EIA, FRED and OECD data)

Figure 1.1 presents a visual overview of the main variables used throughout the thesis. The co-movement between global activity and crude oil prices is striking, especially during episodes such as the 2003–2008 expansion and the COVID-19 contraction. Production

adjusts slowly, while inventories exhibit spikes during periods of heightened uncertainty. These stylised facts motivate the adoption of a multivariate dynamic model capable of accounting for these interactions.

1.2 Problem Statement

Despite extensive research, economists and practitioners face several persistent challenges in modelling and interpreting oil price dynamics.

First, the oil market is inherently multivariate. Real oil prices respond to production, global business cycles, inventory adjustments and financial market conditions. Univariate models, including autoregressive specifications and static regressions, cannot reproduce these joint dynamics. Formal diagnostic tests confirm the inadequacy of such models: regressions of the real price of oil on production, activity and inventories exhibit strong serial correlation in the residuals [18], heteroscedasticity [6] and clear departures from normality [12, 20]. Coefficient instability across subsamples further suggests that relationships are time-varying and regime-dependent [7, 2].

Second, reduced-form VARs, while effective in capturing dynamic interactions, do not provide economically meaningful interpretations of shocks unless a structural identification strategy is imposed. As emphasised by Sims [25] and formalised in the oil-market context by Kilian [14], theory-based restrictions are essential for distinguishing supply, aggregate-demand and precautionary-demand innovations. Building on these principles, Rubio-Ramirez, Waggoner, and Zha [24] show how identification schemes can be derived in a fully Bayesian framework. Without economically motivated restrictions, impulse responses cannot be interpreted in terms of underlying structural mechanisms.

Third, extreme events play a central role in the oil market. Structural shocks display heavy-tailed distributions, meaning that rare but impactful events occur with higher probability than implied by Gaussian models. Modelling these extremes requires flexible distributional assumptions and tools capable of capturing tail dependence, such as copulas [21, 22].

Finally, translating structural oil shocks into industrial risk metrics requires bridging two domains: macroeconometric modelling and corporate finance. Firms need tools that not only identify the origins of price movements, but also translate them into actionable scenarios, stress tests and hedging implications. This is particularly relevant for airlines, where fuel-price risk affects fleet planning, pricing strategies and financial performance.

1.3 Theoretical Framework

The theoretical backbone of this thesis is the structural VAR framework originally proposed by Kilian [14] and later refined by Kilian and Murphy [15]. In this framework, the global oil market is driven by three fundamental shocks:

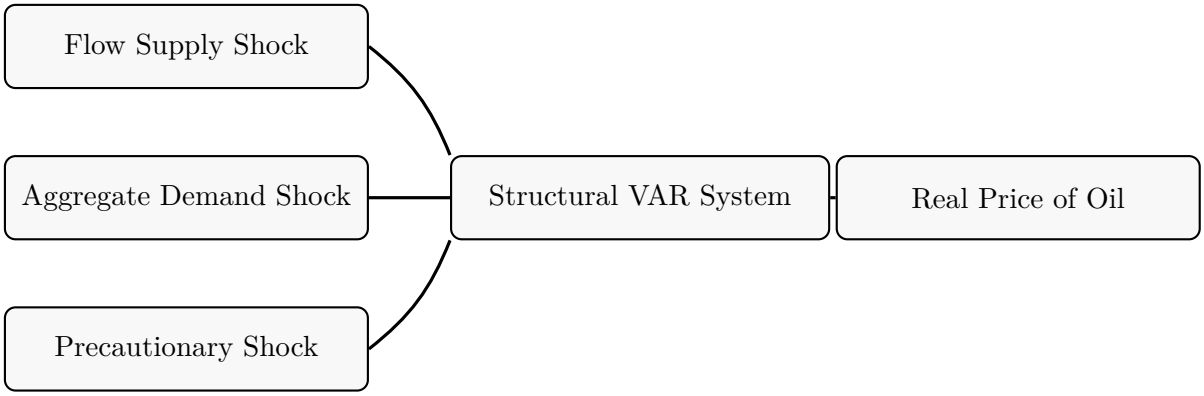

Figure 1.2: Conceptual structure of the oil market SVAR model.

1. **Flow supply shocks** — unexpected changes in global crude oil production.
2. **Aggregate demand shocks** — shifts in global real economic activity, reflecting industrial demand for commodities.
3. **Precautionary or inventory demand shocks** — changes in expectations about future oil availability, inferred through adjustments in inventories.

Flow supply shocks typically have limited and short-lived effects on oil prices due to the inelasticity of near-term production. By contrast, aggregate demand shocks produce large and persistent price movements, reflecting the procyclical nature of industrial commodity markets. Precautionary demand shocks capture periods of heightened uncertainty, during which firms and speculators increase inventory holdings in anticipation of potential future shortages[14, 5].

Figure 1.2 provides a schematic representation of the structural model. Each shock affects oil prices through distinct channels, though real-world dynamics often involve interactions between shocks. The structural VAR allows researchers to quantify these effects through impulse response functions (IRFs) and forecast error variance decompositions (FEVD).

Beyond the VAR, this thesis incorporates distributional analysis of structural shocks, building on the observation that heavy tails and nonlinear dependence are key features of global commodity markets. Understanding tail dependencies is crucial for designing robust stress tests and risk scenarios.

1.4 Research Objectives

This thesis pursues four overarching objectives:

1. **To construct a harmonised and comprehensive monthly dataset (1990–2024)** including real crude oil prices, global crude oil production, OECD industrial

activity and U.S. petroleum and product inventories, using official sources such as the EIA and the Federal Reserve [29, 31, 32].

2. **To estimate and validate a reduced-form VAR model** that captures the dynamic interactions between these variables, supported by extensive diagnostic testing [19].

3. **To identify structural shocks using sign restrictions and elasticity bounds**, following the methodology of Kilian and Murphy [15], and to characterise their impulse responses and variance contributions.

4. **To translate structural oil shocks into industrial risk metrics**, including Monte Carlo scenario generation, Hormuz-type stress testing and hedging implications for a commercial airline exposed to jet fuel price fluctuations.

1.5 Methodological Contribution

This thesis makes several methodological contributions to the empirical analysis of oil markets and their industrial applications:

- **Data construction and proxy evaluation.** It provides a harmonised dataset covering more than three decades of global oil market activity. A key contribution is the evaluation of alternative proxies for global real activity, comparing OECD-based indicators to the *REA* index [9, 13].

- **Structural identification.** The thesis implements a robust identification strategy based on sign and elasticity restrictions, ensuring economically meaningful structural shocks consistent with the oil market literature [15, 5].

- **Distributional characterisation of shocks.** It documents heavy-tailed marginal distributions and copula-based dependence structures across structural shocks, revealing substantial tail dependence between demand and precautionary disturbances [21, 22].

- **Stress-testing framework.** The thesis develops a scenario generation and stress-testing framework grounded in structural econometrics and applicable to industrial decision-making, particularly the aviation sector.

- **Application to fuel risk management.** The thesis bridges macroeconomic modelling with corporate risk management by mapping structural oil shocks into jet fuel price paths and assessing the impact on an airline's fuel cost exposure.

Table 1.1: Key structural mechanisms in oil markets.

Mechanism	**Description**	**References**
Flow supply	Slow adjustment due to extraction and investment constraints	Kilian & Murphy (2014)
Aggregate demand	Driven by the global business cycle and industrial activity	Barsky & Kilian (2002, 2004)
Inventory demand	Reflects expectations about future availability	Alquist, Bhattarai & Coibion (2019)
Speculation	Amplifies short-run volatility	Sockin & Xiong (2015)

1.6 Structure of the Thesis

The thesis is organised into five chapters:

- **Chapter 2** introduces the dataset, details preprocessing steps and presents the econometric methodology, including stationarity analysis and the specification of the reduced-form VAR model.
- **Chapter 3** presents the estimation results of the VAR model and the identification of structural shocks. It reports impulse responses, variance decompositions and the transmission of shocks to oil prices.
- **Chapter 4** examines the empirical distributions of structural shocks, estimates copula models to capture nonlinear dependence and applies the structural results to scenario generation, stress testing and hedging.
- **Chapter 5** concludes by summarising the main findings, discussing limitations and proposing avenues for future research.

These considerations motivate the multivariate modelling framework employed in the remainder of this thesis.

Chapter 2

Data and Econometric Methodology

2.1 Overview

This chapter documents the construction of the dataset and the econometric framework that underpins the empirical analysis of the oil market and the subsequent stress–testing and hedging applications. The objective is twofold. First, to provide a transparent account of each transformation applied to the raw data, so that the analysis can be replicated and extended. Second, to show why a multivariate dynamic specification — in particular a structural vector autoregression (SVAR) — is required to model the joint behaviour of oil prices, U.S. production, OECD activity and inventories, instead of static regression models.

The empirical work is based on monthly data from January 1990 to December 2024. The data are sourced from standard repositories in the energy economics literature: the Federal Reserve Bank of St. Louis (FRED), the U.S. Energy Information Administration (EIA), the Dallas Fed Globalization Institute and OECD statistics.[1] All series are imported, cleaned and merged by the MATLAB script `build_oil_dataset.m`, which creates three core objects:

(i) a timetable `All` containing the main variables in levels (nominal and real), at a common monthly frequency;

(ii) a timetable `All_d` with stationary transformations (log-differences and standardised cycles) used in the pre–VAR diagnostics;

(iii) a timetable `ALL_VAR` with the transformed variables entering the structural VAR.

Figure 2.1 anticipates the final VAR variables, while the remaining figures in this chapter summarise the unit root and diagnostic tests, the lag selection and the in-sample

[1] See U.S. Energy Information Administration [29], U.S. Bureau of Labor Statistics [28], Federal Reserve Bank of Dallas [9], and U.S. Energy Information Administration [32, 31, 30] for the official documentation of the underlying series.

fit of the VAR model. Tables 2.1–2.5 report the corresponding numerical results.

2.2 Data Sources

2.2.1 Real WTI Crude Oil Price

The benchmark price variable is the West Texas Intermediate (WTI) spot price at Cushing, Oklahoma, obtained from the FRED series `MCOILWTICO`.[2] The original data are quoted in U.S. dollars per barrel and correspond to monthly averages of daily prices. To account for inflation, nominal WTI prices are deflated by the U.S. Consumer Price Index for All Urban Consumers (CPI-U, series `CPIAUCSL`).[3] The real price index is constructed as

$$\mathrm{WTI}_t^{\mathrm{real}} = 100 \times \frac{\mathrm{WTI}_t^{\mathrm{nom}}}{\mathrm{CPI}_t},$$

so that the base value of the index is 100 in the first observation of the sample. This transformation is consistent with the treatment of real oil prices in Kilian [14], Kilian and Murphy [15], and Baumeister and Hamilton [5].

Although Brent is often employed as the benchmark for global crude oil pricing, this study adopts the real WTI price as the reference series. This choice is consistent with the U.S.-centred nature of the dataset — which combines WTI prices with U.S. production and inventory data — and with the focus on risk management for an airline hedging exposures linked to WTI-denominated futures and spot prices. The reliance on WTI rather than Brent implies that the resulting price dynamics are most directly informative for the U.S. oil market; this limitation is discussed further in the concluding chapter.

2.2.2 U.S. Crude Oil Production

The production variable is used to proxy the flow supply of crude oil. In the baseline dataset, production is measured using monthly U.S. crude oil output from the EIA International Energy Statistics, expressed in thousand barrels per day.[4] U.S. production is a natural driver of WTI dynamics because the benchmark is physically delivered in the United States and domestic supply responds strongly to technological and regulatory shifts, such as the shale oil expansion in the mid-2000s.

Unlike Kilian and Murphy [15], who rely on world crude oil production as a measure of global flow supply, this study uses U.S. output as the supply indicator. Consequently, the identified supply disturbance in the SVAR should be interpreted as a U.S.-centred WTI-market supply shock rather than as a fully global flow supply shock. This U.S. focus is consistent with the broader dataset design, which combines WTI prices with U.S. production and inventory data.

[2] See U.S. Energy Information Administration [29].
[3] See U.S. Bureau of Labor Statistics [28].
[4] See U.S. Energy Information Administration [32] for the reference to the EIA production series.

Following the literature on oil market VAR models, production enters the structural specification in logarithms, allowing shocks to be interpreted as percentage changes in supply [15, 16].

2.2.3 OECD Industrial Activity

Global demand conditions are proxied by an index of industrial activity for the OECD aggregate. The underlying series is an industrial production index compiled by OECD, with base year equal to 2015 and monthly frequency. In the early SVAR literature, global demand for industrial commodities is typically measured by the Kilian index of global real economic activity (REA), built from ocean freight rates [14]. However, subsequent work has highlighted several shortcomings of REA, including sensitivity to shipping market reforms, structural breaks around China's WTO accession and limited information content in the post-2010 period [13, 16]. In the present dataset, REA-based specifications display weaker statistical properties than OECD industrial activity: OLS regressions with REA produce less stable coefficients and more severe residual autocorrelation relative to OECD, and VAR models with REA show poorer diagnostics. For these reasons, OECD is adopted as a more robust proxy for global demand conditions in the identification of aggregate demand shocks, in line with the recent re-assessment of demand indicators in Kilian [13].

2.2.4 U.S. Oil Inventories

Crude oil and refined product inventories play a central role in models where precautionary demand and speculative storage link expectations about future scarcity to current prices [15, 5]. Inventory data are obtained from the EIA's International Energy Database as the total end-of-period stocks of crude oil and petroleum products in the United States.[5] The data are expressed in million barrels and reported at monthly frequency. As discussed in Kilian and Murphy [15], it is not the level of inventories per se but unexpected changes in stocks that identify precautionary demand shocks. Consequently, in the structural VAR inventories are transformed to logarithms and subsequently filtered to obtain stationary deviations around trend.

2.2.5 Jet Fuel Prices (U.S. Gulf Coast)

For the hedging application in later chapters, jet fuel prices are also required. The relevant series is the kerosene-type jet fuel spot price at the U.S. Gulf Coast, expressed in dollars per gallon and reported at monthly frequency by the EIA.[6] These data are imported and stored in the variable `JetFuel_USGC` in `All`. While jet fuel does not enter the VAR directly, it is linked to real WTI prices through a pass-through regression in the hedging module.

[5] See U.S. Energy Information Administration [31].
[6] See U.S. Energy Information Administration [30].

2.2.6 Inflation Measure and Deflation

The CPI-U index serves both as a deflator for nominal oil prices and as a proxy for general price-level movements in the U.S. economy [28]. After reshaping the CPI series to monthly frequency and aligning the date conventions, the `build_oil_dataset.m` script constructs the real WTI series and then discards the nominal WTI to avoid redundancy. The CPI series itself does not enter the VAR system but is retained for consistency checks and potential extensions involving real interest rates or inflation dynamics.

2.2.7 Summary of Data Sources

A detailed description of data construction, frequency alignment and pre-VAR diagnostics is provided in Appendix A.

Table 2.1 summarises all variables employed in the analysis, their definitions, units of measurement and original sources.

Table 2.1: Data sources and variable definitions.

Variable	**Definition**	**Source**	**Frequency**
WTI_real	Real West Texas Intermediate crude oil price (index, 1990=100)	FRED, EIA [29]	Monthly
Production	U.S. crude oil production (thousand barrels per day)	EIA [32]	Monthly
OECD (IPI)*	OECD industrial activity indicator, Dallas Fed	OECD, Dallas Fed [9, 13]	Monthly
Inventories	U.S. crude oil and petroleum product ending stocks (million barrels)	EIA [31]	Monthly
JetFuel_USGC **	Kerosene-type jet fuel spot price, U.S. Gulf Coast (USD per gallon)	EIA [30]	Monthly
CPI **	Consumer Price Index for All Urban Consumers (1982–84=100)	BLS/FRED [28]	Monthly

* Industrial Production Index

** They are not part of the core VAR system but are needed for the hedging module / deflation and consistency checks

2.3 Preprocessing and Data Harmonisation

All data management is implemented in `build_oil_dataset.m`. The goal is to harmonise the series in terms of time index, frequency and numeric format, and to prepare both stationary and non-stationary transformations consistent with the subsequent VAR specification.

2.3.1 Date Alignment and Monthly Frequency

Source files differ in their original date conventions: some use calendar dates ("yyyy-mm-dd"), others indicate only year and month ("yyyy-mm"), and some rely on textual month labels. Each series is first converted to a `table` with explicit date and value columns and then mapped to a `datetime` vector using appropriate input formats and locale settings, so that heterogeneous date formats and locales are harmonised in a consistent way. All dates are shifted to the first day of the corresponding month to ensure that the time index is strictly monthly and comparable across series.

The individual series are then recast as `timetable` objects and synchronised by intersecting their support, so that the common sample only retains months in which all variables are observed. This procedure implicitly drops months with missing entries in at least one series and yields a balanced panel of monthly observations from 1990:1 to 2024:12.

2.3.2 Numeric Cleaning

Many of the raw files encode numbers using commas as thousands separators or as decimal separators, depending on the local convention. To avoid parsing issues, all numeric entries are first converted to strings and then cleaned with a simple regular-expression routine that removes non-numeric separators before being cast to double precision. This ensures that subsequent arithmetic operations produce consistent results and that no artefacts arise from locale-specific decimal formats.

2.3.3 Transformations and Construction of `All_d` and `ALL_VAR`

After converting the nominal WTI series into real terms using the CPI deflator, the dataset `All` stores the variables at cleaned monthly frequency: `WTI_real`, `Production`, `OECD`, `Inventories`, `JetFuel_USGC` and `CPI`. Two parallel transformations are then implemented in MATLAB.

Stationary transformations for VAR and preliminary diagnostics. All series intended for OLS, unit root analysis and VAR estimation are transformed into stationary representations. In particular,

$$\begin{aligned}
\Delta \log \mathrm{WTI}_t^{\mathrm{real}} &= \log \mathrm{WTI}_t^{\mathrm{real}} - \log \mathrm{WTI}_{t-1}^{\mathrm{real}}, \\
\Delta \log \mathrm{Prod}_t &= \log \mathrm{Prod}_t - \log \mathrm{Prod}_{t-1}, \\
\Delta \log \mathrm{Inv}_t &= \log \mathrm{Inv}_t - \log \mathrm{Inv}_{t-1}, \\
\Delta \mathrm{OECD}_t &= \mathrm{OECD}_t - \mathrm{OECD}_{t-1}.
\end{aligned}$$

All differenced series are then standardised to zero mean and unit variance, and stored in the structure `All_d` with the suffix `_DL` (`WTI_real_DL`, `Production_DL`, `OECD_DL`, `Inventories_DL`, `JetFuel_DL`). These stationary z–score transforms are used in the pre–

VAR OLS regressions, unit root tests, rolling-window diagnostics (Section 2.5) and, crucially, as inputs for the reduced-form VAR.

VAR state vector and construction of `ALL_VAR`. In line with the econometric evidence in Section 2.4, the reduced-form VAR is estimated directly on the stationary $\Delta \log$ (or difference) transforms, rather than on log levels. The four-dimensional state vector is defined as

$$y_t = \begin{bmatrix} \text{Production\_DL}_t \\ \text{OECD\_DL}_t \\ \text{WTI\_real\_DL}_t \\ \text{Inventories\_DL}_t \end{bmatrix},$$

where the ordering reflects the economic structure of the oil market: flow supply, aggregate demand, spot price and precautionary/storage demand.[7] For convenience, these four series are stacked in the matrix `ALL_VAR`, which contains the stationary, standardised VAR data used in all subsequent estimations.

Figure 2.1 reports the trajectories of the VAR variables in $\Delta \log$ (or difference) form, rescaled to zero mean and unit variance. The four transformed series display pronounced low-frequency swings and episodic extremes (2008 crisis, COVID-19, major geopolitical shocks), but no visible drift, consistent with the unit root behaviour in levels documented in Section 2.4.

2.4 Stationarity and Unit Root Tests

Before specifying the VAR in log levels, it is necessary to assess the order of integration of each series and ensure that the resulting system is econometrically well behaved. Standard unit root tests are therefore applied to both the original level series stored in `All` and to the stationary transformations in `All_d`.

Augmented Dickey–Fuller (ADF) tests are run for each variable in levels, including a constant and a linear trend. For the real WTI price, production and inventories, the unit root null cannot be rejected at conventional significance levels, in line with the literature documenting non-stationarity in real oil prices and macroeconomic aggregates. In contrast, the OECD activity index appears trend–stationary, with the ADF statistic rejecting the unit root null at the 1% level (Table 2.2). Given the mixed evidence and for consistency across variables, the subsequent analysis is conducted on transformed series.

[7] This ordering is maintained throughout the analysis: reduced-form VAR, Cholesky benchmark identification and the sign-restricted SVAR in Chapter 3.

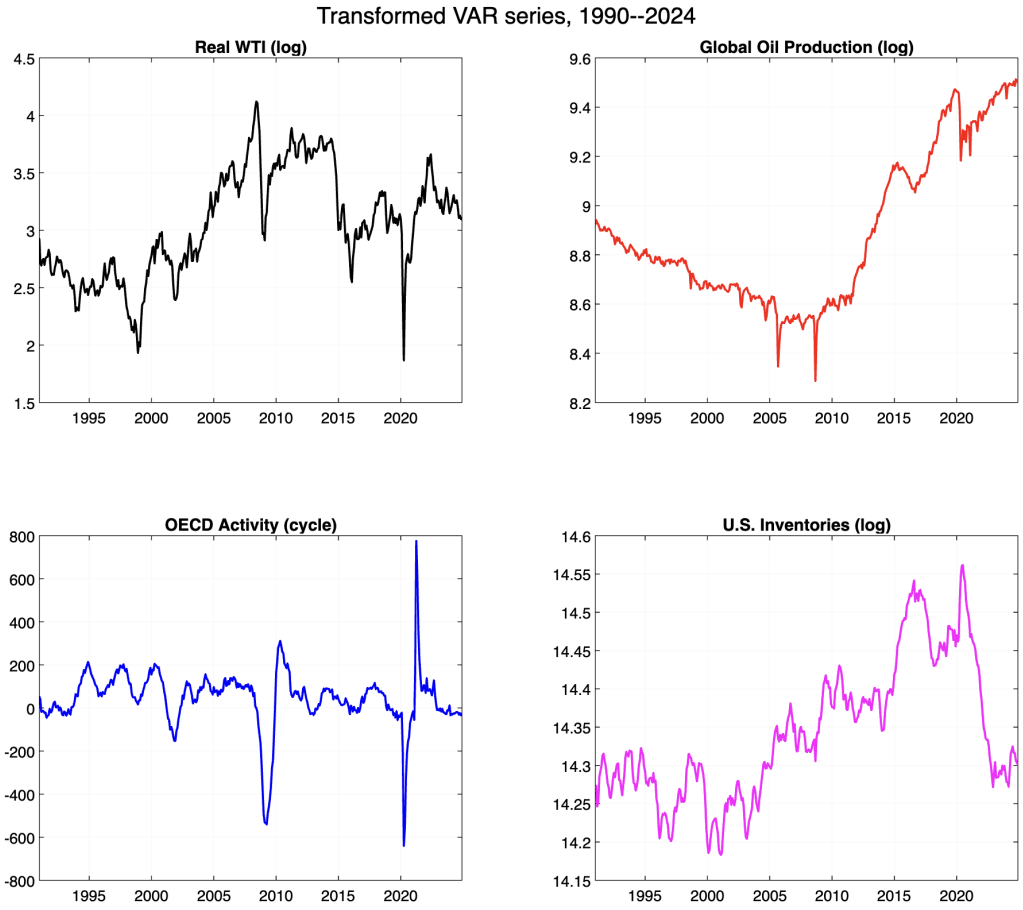

Figure 2.1: Stationary VAR series, 1990–2024. The panels display the standardised Δ log real WTI price, Δ log crude oil production, Δ OECD industrial activity and Δ log petroleum inventories (all series transformed to zero mean and unit variance).

Table 2.2: ADF unit root tests for variables in levels.

Series	**Specification**	**ADF statistic**	**p-value**
WTI_real	constant + trend	-2.083	0.5514
Production	constant + trend	-1.461	0.8411
OECD	constant + trend	-4.060	0.0082
Inventories	constant + trend	-1.020	0.9388

When the same tests are applied to first differences (or, for OECD activity, to the cyclical component), the unit root null is strongly rejected for all series, with p-values around 0.001, as shown in Table 2.3. Given the strong evidence of unit roots in the level series, the VAR is specified in terms of stationary log-differences (and, for OECD activity, detrended cyclical components). This choice eliminates stochastic trends from the state vector and preserves the validity of standard VAR inference without imposing explicit

cointegration restrictions. Long-run effects on the levels of the variables are then recovered by cumulating the impulse responses of log-differences, as discussed in Chapter 3.

Table 2.3: ADF unit root tests for transformed series.

Series	**Specification**	**ADF statistic**	**p-value**
WTI_real_DL	constant	-15.863	0.0010
Production_DL	constant	-23.385	0.0010
OECD_DL / OECD_cycle	constant	-14.844	0.0010
Inventories_DL	constant	-13.960	0.0010

Additional test statistics and residual diagnostics are reported in Appendix A.

2.5 Exploratory OLS Evidence and Limitations

As a preliminary step, static regression models are estimated to gauge whether simple linear relationships between real oil prices and fundamentals can adequately describe the data. These regressions are implemented in `ols_prevar_check.m` and form the basis for arguing in favour of a dynamic multivariate specification.

2.5.1 Baseline Static Regression

As a starting point, a simple static specification relates the log real WTI price to fundamental variables in levels. Specifically,

$$\log \mathrm{WTI}_t^{\mathrm{real}} = \alpha + \beta_1 \log \mathrm{Prod}_t + \beta_2 \mathrm{OECD}_t + \beta_3 \log \mathrm{Inv}_t + u_t,$$

where all regressors enter contemporaneously and no lags are included. In line with Kilian [14] and Baumeister and Hamilton [5], this static log–linear regression explains only a limited share of the variation in real oil prices: the adjusted R^2 remains modest, and the residuals display serial correlation, heteroskedasticity and non–normality, as indicated by the Ljung–Box Q-statistic, the Breusch–Pagan test and the Jarque–Bera normality test reported in Table 2.4. These diagnostics highlight that a purely contemporaneous specification is inadequate and motivate the move to a multivariate dynamic VAR framework.

Table 2.4: Diagnostic tests for static OLS regression of real WTI.

Test	**Statistic**	**p-value**	**Conclusion**
Ljung–Box (12 lags)	34.41	0.0006	serial correlation present
Breusch–Pagan	27.74	0.0000	heteroscedasticity present
Jarque–Bera	197.17	< 0.001	residuals non-normal

2.5.2 Structural Instability and Rolling Windows

To assess the stability of the OLS relationship over time, `ols_windows.m` re-estimates the static regression on rolling subsamples (e.g. 10- or 15-year windows). The resulting sequences of coefficients reveal substantial time variation: production and inventory elasticities change sign across subsamples, and the effect of OECD on real WTI becomes weaker or stronger depending on the period. This is consistent with evidence from structural break tests such as those of Brown, Durbin, and Evans [7] and Bai and Perron [2], which typically identify multiple breakpoints in macroeconomic relationships over the last four decades.

The instability of static coefficients, combined with unsatisfactory residual diagnostics, confirms that the oil market is governed by dynamic interactions and time-varying responses. This motivates the move to a VAR framework, where lagged dependencies and feedback effects can be explicitly modelled.

2.6 VAR Model Specification

2.6.1 Reduced-Form VAR

The baseline multivariate model is a reduced-form VAR in log levels (for oil prices, production and inventories) and in levels for OECD activity:

$$y_t = c + A_1 y_{t-1} + \cdots + A_p y_{t-p} + u_t,$$

where $y_t = (\text{OECD\_level}_t, \text{Prod\_log}_t, \text{WTI\_log}_t, \text{Inv\_log}_t)'$, c is a vector of intercepts, A_i are 4×4 lag matrices, and u_t is a vector of reduced-form innovations with covariance matrix Σ_u. The model is estimated by ordinary least squares equation-by-equation, which is efficient under the assumption of Gaussian errors and homoscedasticity [25, 19].

The choice of working with log levels — as opposed to differenced series — follows the practice in the structural oil market literature and allows for the possibility of long-run co-movements between oil prices and fundamentals [14, 5]. At the same time, a sufficiently rich lag structure is included to ensure that the VAR residuals are approximately white noise and that the system is dynamically stable. A detailed description of the reduced-form VAR specification, lag selection and stability diagnostics is provided in Appendix B.

2.6.2 Lag Length Selection

Lag length is selected empirically by combining dynamic stability and residual whiteness. In the `var_main.m` script, a sequence of VAR(p) models with $p = 1, \ldots, 15$ is estimated, and for each specification two diagnostics are recorded: (i) whether all eigenvalues of the companion matrix lie inside the unit circle and (ii) the minimum p-value of a Ljung–Box portmanteau test for serial correlation in the residuals of the real WTI equation, based on the stationary representation in `All_d`. The results are summarised in Table 2.5.

Table 2.5: Empirical VAR lag selection based on stability and Ljung–Box test on residuals (`All_d`, equation for real WTI).

Lag p	**Stable**	**min** LB p**-value**
1	Yes	0.0000
2	Yes	4.65×10^{-13}
3	Yes	9.61×10^{-12}
⋮	⋮	⋮
11	Yes	2.92×10^{-8}
12	Yes	0.7523
13	Yes	0.5111

Note: Although only selected lag orders are reported, all VAR(p) specifications up to $p = 15$ are dynamically stable. For $p \leq 11$ the minimum Ljung–Box p-values are effectively zero, indicating strong residual autocorrelation. Starting from $p = 12$, the p-values exceed conventional significance thresholds, signalling that remaining serial dependence is modest. On this basis, a VAR(12) is adopted as the baseline specification.

All VAR(p) specifications turn out to be dynamically stable. However, for $p \leq 11$ the Ljung–Box p-values are effectively zero, indicating strong residual autocorrelation and insufficient dynamic structure. Starting from $p = 12$, the portmanteau p-values exceed conventional significance thresholds, signalling that the remaining serial dependence is modest and compatible with a well-specified VAR.

On this basis, a VAR(12) is adopted as the baseline specification. This choice is also consistent with the monthly frequency of the data and with the lag length commonly used in the structural oil market literature [14, 15], while preserving a reasonable number of degrees of freedom for estimation and subsequent structural analysis.

2.6.3 Residual Diagnostics and Stability

After estimating the VAR(12), standard diagnostics are carried out to ensure that the reduced-form specification is adequate. Portmanteau tests for serial correlation in the residuals confirm that the dynamic structure absorbs most temporal dependence, with no evidence of remaining autocorrelation at conventional lags. Tests for normality based on Jarque–Bera and Kolmogorov–Smirnov statistics, applied to the standardized residuals, reveal departures from Gaussianity and some signs of heteroscedasticity, which is not surprising given the presence of large oil price swings and episodic volatility clustering. Nevertheless, the VAR residuals are sufficiently well behaved for the purpose of structural identification and impulse response analysis.

Stability is examined by inspecting the eigenvalues of the companion matrix: all lie strictly inside the unit circle, confirming that the VAR is dynamically stable. This property is crucial for the interpretation of impulse responses and for the generation of stress-test scenarios in later chapters.

2.6.4 In-Sample Fit

To provide a sense of how well the VAR captures the dynamics of the real oil price, the script `var_fit_vs_actual_WTI.m` computes one-step-ahead in-sample forecasts for the VAR(12) and compares the fitted values of `WTI_log` with the observed series. Figure 2.2 plots the actual and fitted values. The VAR tracks medium-run movements in real WTI reasonably well, including the run-up in the early 2000s, the collapse during the global financial crisis, and the shale-driven adjustments in the 2010s. Short-lived spikes and collapses are not perfectly matched, reflecting the limits of linear Gaussian models in capturing extreme events, but the overall fit is markedly superior to that of the static OLS regression in Section 2.5.

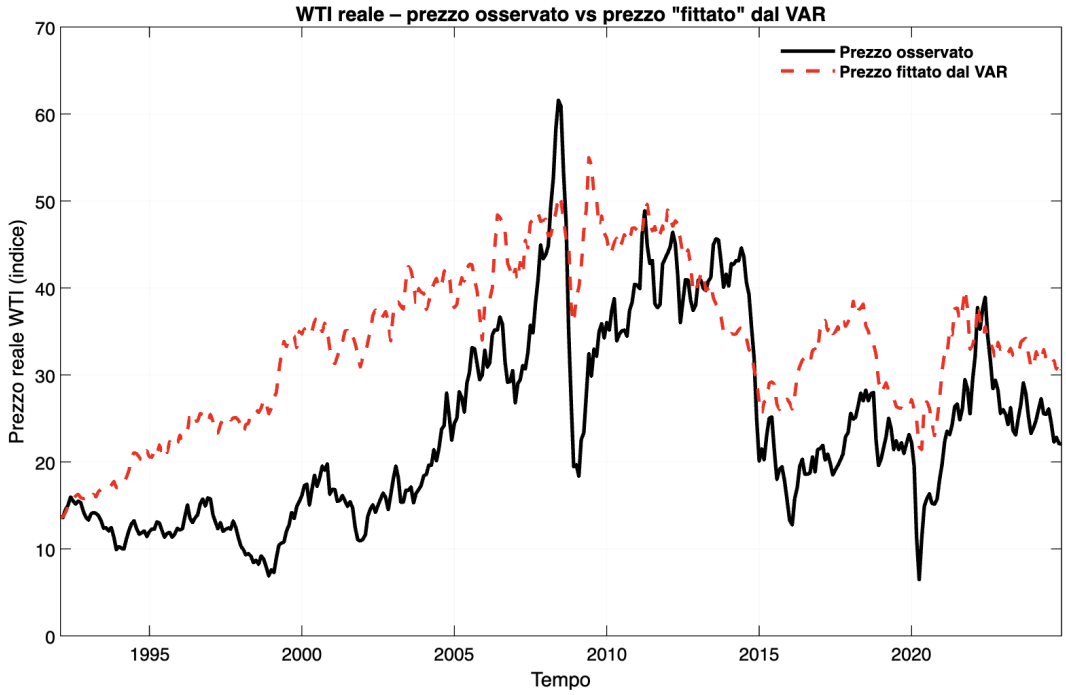

Figure 2.2: In-sample VAR(12) fit vs actual log real WTI price. The VAR captures medium-run fluctuations in the real oil price, while short-lived extremes remain harder to match.

2.7 Structural Identification Strategy

The reduced-form VAR alone does not provide economically meaningful interpretations of shocks, since the innovations u_t are linear combinations of underlying structural disturbances. Following the oil market literature, the thesis adopts a structural VAR (SVAR) approach with sign and elasticity restrictions to identify three economically interpretable shocks: a (US-centred) flow supply shock, an aggregate demand shock and a precautionary (inventory) demand shock [14, 15, 5].

Let ε_t denote the vector of structural shocks, and B the contemporaneous impact

matrix such that

$$u_t = B\varepsilon_t, \qquad \Sigma_u = BB'.$$

Identification is achieved by imposing sign restrictions on the impulse responses of y_t to each column of B over a short horizon, combined with bounds on the short-run price elasticities of supply and demand. The procedure builds on the framework and formal identification results of Rubio-Ramirez, Waggoner, and Zha [24]. The specific numerical ranges for the elasticity bounds are reported in Section 3.3.2.

A flow supply shock is required to reduce crude oil production and increase the real oil price on impact, while its effect on inventories is either negative or slightly positive, reflecting the drawdown of stocks in response to supply shortfalls. Since the supply indicator in this thesis is US crude oil output rather than world production, this disturbance is best interpreted as a supply shock to the US WTI market, not as a fully global flow supply shock in the sense of Kilian and Murphy [15]. An aggregate demand shock must increase OECD activity, production and the oil price jointly, consistent with strong global demand for industrial commodities. A precautionary demand shock, in turn, is characterised by an increase in inventories and real oil prices, while its effect on production and OECD activity is more muted [15]. Plausible bounds on the short-run price elasticities of supply and demand further constrain the admissible decompositions of Σ_u.

The actual implementation of sign restrictions is carried out in `svar_sign_restrictions.m`, which draws candidate orthogonal matrices, rotates the Cholesky factor of Σ_u, and retains only those rotations that satisfy the imposed sign and elasticity conditions over the chosen horizon. This yields a distribution of admissible impulse responses rather than a single point estimate, reflecting the partial nature of identification and addressing concerns raised by Baumeister and Hamilton [5] about overconfident structural interpretations.

The identification strategy builds directly on the specification choices documented in this chapter: the selection of OECD activity as a robust demand proxy, the log-level transformation of WTI, production and inventories, and the adoption of a sufficiently rich lag structure to absorb unit root behaviour and short-run dynamics. Without these preparatory steps, the structural analysis in the subsequent chapter would rest on a fragile econometric foundation.

Chapter 3

Empirical Analysis of Oil Market Dynamics

3.1 Overview

This chapter presents the empirical analysis of the oil market based on the multivariate dynamic framework developed in Chapter 2. Building on the harmonised monthly dataset and the VAR(12) specification constructed through `build_oil_dataset.m` and `var_main.m`, the objective is to identify and quantify the structural disturbances driving the real price of oil.

The analysis follows the structural VAR (SVAR) approach of Kilian [14] and Kilian and Murphy [15], using sign and elasticity restrictions to identify three economically meaningful shocks: a flow supply shock, an aggregate demand shock, and a precautionary demand shock. Impulse responses, forecast error variance decompositions (FEVDs) and historical decompositions are used to characterise the transmission of these shocks. The final section maps structural shocks into WTI price trajectories, laying the groundwork for the scenario-based stress tests in Chapter 4.

In addition to the VAR/SVAR analysis reported in this chapter, Appendix B provides an exploratory study of the marginal distributions and copula-based dependence structure of the identified structural shocks.

3.2 Reduced-Form VAR Results

3.2.1 Estimation and Diagnostics

The reduced-form VAR(12) is estimated on the stationary vector

$$x_t = \begin{bmatrix} \Delta \log \mathrm{Prod}_t \\ \mathrm{OECD\_cycle}_t \\ \Delta \log \mathrm{WTI}_t \\ \Delta \log \mathrm{Inv}_t \end{bmatrix},$$

whose components correspond to the standardised transformations `Production_DL`, `OECD_cycle`, `WTI_real_DL` and `Inventories_DL` in `All_d`.

Residual diagnostics for the VAR(12) indicate (Table 2.5, Table 3.1, Figure 3.1 and Appendix B):

- no significant residual autocorrelation, as Ljung–Box portmanteau p-values are well above conventional thresholds;
- all companion-matrix eigenvalues strictly inside the unit circle, confirming dynamic stability;
- mild departures from normality (Jarque–Bera tests) and evidence of heavy tails in the residual distribution of the WTI equation;
- overall, sufficient goodness-of-fit and stability for subsequent structural identification.

Table 3.1: Reduced-form VAR(12) equation fit statistics.

Equation	**Number of Parameters**	**Std. Error**	$\mathbf{R^2}$	**Adj.** R^2
Production_DL	49	0.9358	0.2507	0.1468
OCSE_DL	49	0.7255	0.5493	0.4868
WTI_real_DL	49	0.9620	0.1928	0.0808
Inventories_DL	49	0.8205	0.3978	0.3143

To quantify the in-sample forecasting performance of the reduced-form model, Table 3.2 reports standard accuracy metrics for real WTI, based on the script `var_fit_vs_actual_WTI.m`.

Table 3.2: Accuracy metrics for VAR predicted vs. actual real WTI.

Metric	Value
RMSE	12.28
MAE	10.66
MAPE	61.34%

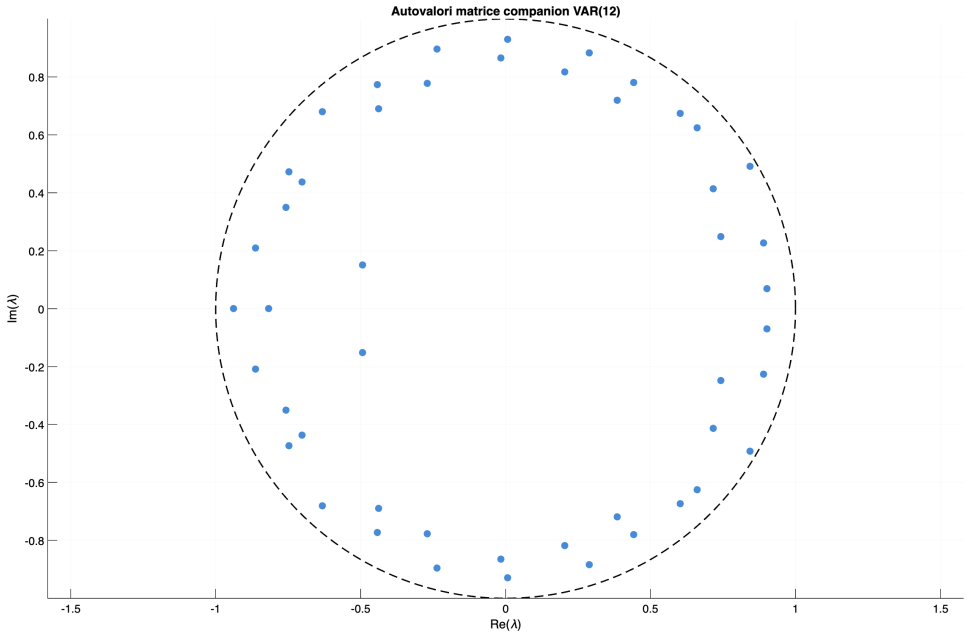

Figure 3.1: Companion matrix eigenvalues for the VAR(12). All lie inside the unit circle.

3.3 Structural Identification via Sign Restrictions

3.3.1 Economic Restrictions

Following Kilian [14] and Kilian and Murphy [15], sign restrictions are imposed over horizons $h = 0, 1, 2$:

- **Flow supply shock:** production ↓, inventories ↓, real WTI ↑, OECD – limited reaction.
- **Aggregate demand shock:** OECD ↑, production ↑, real WTI ↑, inventories ↑.
- **Precautionary demand shock:** inventories ↑, real WTI ↑, OECD ≈ unchanged.

Table 3.3 summarises the full set of restrictions used in the baseline specification.

Table 3.3: Sign restrictions used for structural identification (responses on impact).

Variable	Supply Shock	Aggregate Demand Shock	Precautionary Shock
Production	−	+	0
OECD_cycle	0	+	0
Inventories	−	+	+
Real WTI	+	+	+

3.3.2 Elasticity Bounds

Elasticity constraints follow Kilian and Murphy [15]:

$$\varepsilon_p^s \in [-0.05, 0], \qquad \varepsilon_p^d \in [-0.2, -0.01].$$

These enforce plausible short-run responses of supply and demand to price movements.

3.3.3 Implementation

The routine `svar_sign_restrictions.m` implements the rotation-based procedure of Rubio-Ramirez, Waggoner and Zha[24]. Starting from the reduced-form covariance matrix Σ_u, the algorithm computes its Cholesky factor P, draws random orthonormal matrices Q from the Haar distribution, and constructs candidate impact matrices $B = PQ$. A draw is retained only if the corresponding impulse responses satisfy all sign restrictions over the horizon $h = 0, \ldots, H$; otherwise it is discarded. In the baseline specification, accepted draws represent about 1–3% of all candidates, in line with Kilian and Murphy[15].

3.4 Impulse Response Functions

Because the VAR is estimated on stationary log-differences (and on the detrended OECD activity index), the raw impulse responses describe the effect of each structural shock on monthly growth rates. For economic interpretation, impulse responses for the levels are obtained by cumulating the responses of log-differences over the horizon. The figures reported in this section refer to these cumulated responses and can therefore be read as percentage deviations of the levels from their baseline paths.

Impulse responses (IRFs) are computed over a 36-month horizon using bootstrap percentile bands. For each shock, we report the median and the 16th–84th percentiles across accepted structural decompositions.

Table 3.4 summarises the basic distributional properties of the identified shocks, confirming that they are approximately mean-zero and exhibit non-Gaussian higher moments.

Table 3.4: Descriptive statistics of identified structural shocks.

Shock	**Mean**	**Std. Dev.**	**Skewness**	**Kurtosis**
Supply	0.0000	1.0013	0.0973	3.6076
Aggregate Demand	0.0000	1.0013	−0.5293	4.7428
Precautionary	0.0000	1.0013	1.7476	16.5490

3.4.1 Flow Supply Shock

A negative flow supply shock — interpreted as an unanticipated shortfall in U.S. crude oil production — generates the following pattern in the cumulated responses:

- an immediate rise in the real WTI price, peaking after roughly 3–4 months before gradually declining;

- a decline in crude oil production on impact, with only partial recovery over the subsequent year;
- an inventory drawdown consistent with the use of stocks to smooth the temporary supply shortfall;
- a muted and statistically imprecise reaction in OECD activity.

This configuration is qualitatively consistent with the supply-driven oil price episodes documented by Kilian [14].

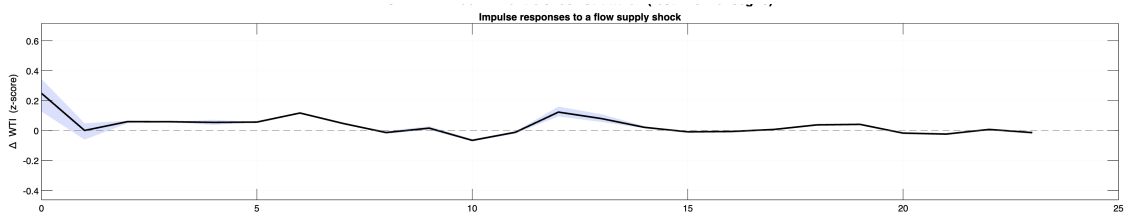

Figure 3.2: Impulse responses to a flow supply shock.

3.4.2 Aggregate Demand Shock

An aggregate demand expansion, capturing shifts in global economic activity, produces:

- a strong and persistent rise in OECD activity;
- an increase in crude oil production and inventories, reflecting the response of supply and stock-building to stronger demand;
- a sustained increase in the real WTI price that remains positive for roughly 12–18 months.

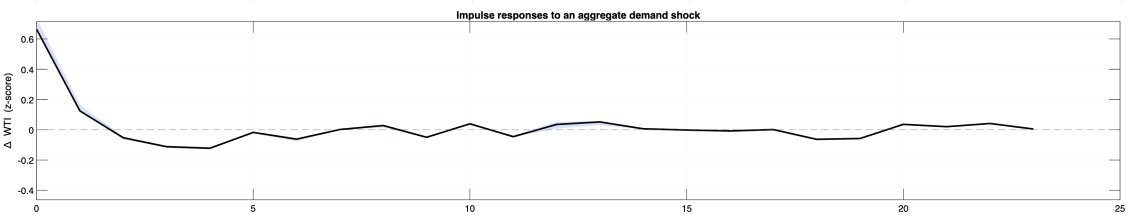

Figure 3.3: Impulse responses to an aggregate demand shock.

3.4.3 Precautionary Demand Shock

A precautionary demand shock — interpreted as a revision in expectations of future scarcity — yields:

- an immediate and sizeable increase in inventories, as market participants build precautionary stocks;

- a short-lived but sharp increase in the real WTI price, which peaks within a few months and then dissipates;
- negligible and statistically weak effects on OECD activity and crude oil production.

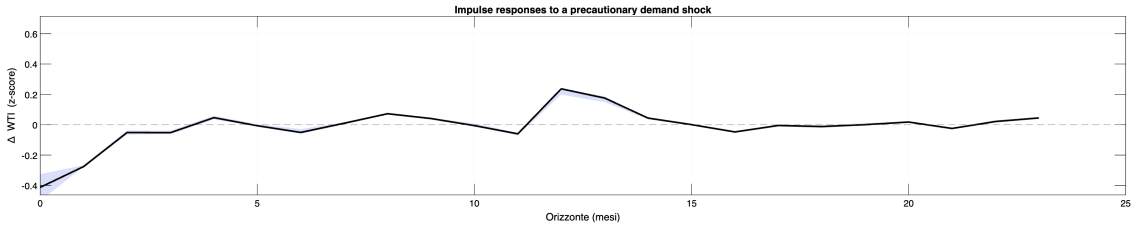

Figure 3.4: Impulse responses to a precautionary demand shock.

3.5 Forecast Error Variance Decomposition

The FEVD quantifies the importance of each shock in explaining forecast error variance at different horizons. Results are consistent with Kilian [14] and Baumeister and Hamilton [5]:

- supply shocks: limited contribution at short horizons;
- aggregate demand shocks: dominant at 6–18 months;
- precautionary shocks: relevant for short-run volatility.

3.5.1 Multipanel FEVD Overview

To provide a compact view of the contribution of each structural shock to the variability of the real WTI price, Figure 3.5 reports the SVAR-based forecast error variance decomposition over horizons up to 24 months. Aggregate demand shocks account for roughly 45–50% of the forecast error variance at horizons between 6 and 18 months, while flow supply and precautionary shocks each explain about 10% in the long run.

The identification scheme and the main properties of the structural shocks are summarised in Appendix B.

3.6 Historical Decomposition

Historical decomposition assigns each observed movement in real WTI to one of the structural shocks. Using `extract_structural_shocks.m`, contributions are reconstructed across the full sample.

The decomposition indicates:

- 2003–2008 oil price surge: predominantly aggregate demand;

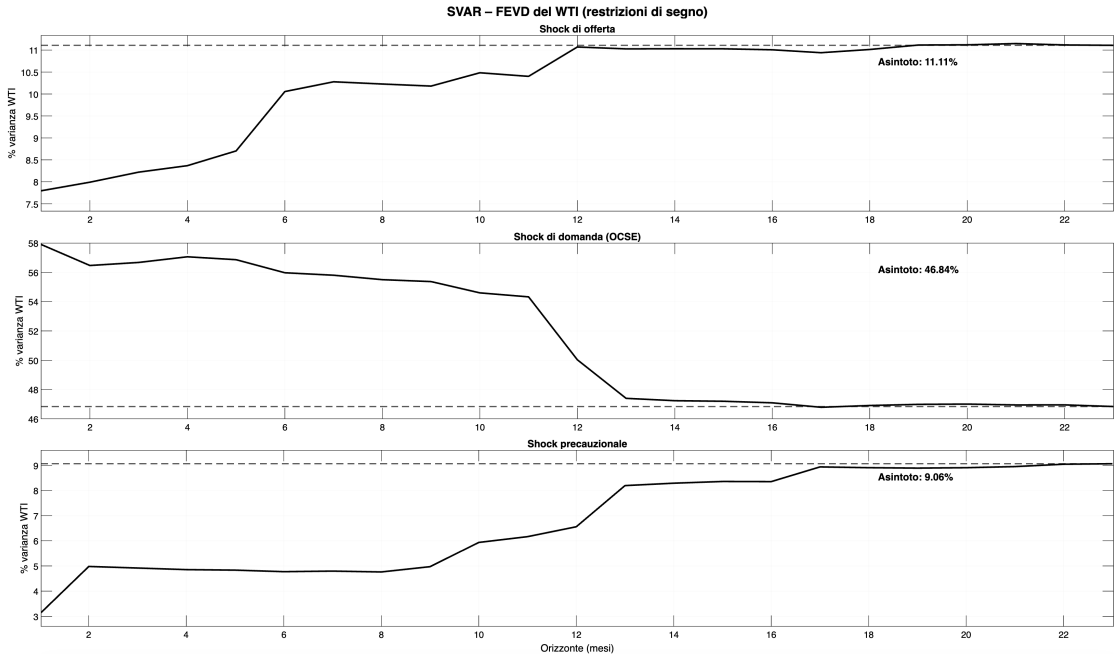

Figure 3.5: SVAR-based forecast error variance decomposition of the real WTI price by structural shock (flow supply, aggregate demand, precautionary).

- 2008 collapse: fall in aggregate demand + unwinding of precautionary positions;
- 2014–2016 decline: persistent positive supply shocks (shale expansion).

3.7 Mapping Structural Shocks to Price Trajectories

To generate the scenario-based projections in Chapter 4, structural shocks must be translated into paths for the level of the real WTI price. Since the VAR is estimated on stationary log-differences, the impulse responses are first cumulated to obtain the effect of each shock on the log level of the real price.

Let $\theta_h^{(j)}$ denote the *cumulated* impulse response of log real WTI at horizon h to a unit structural shock $j \in \{s, d, p\}$ (flow supply, aggregate demand, precautionary). For a shock of magnitude ε_j, the deviation of log real WTI from its baseline path at horizon h is

$$\Delta \log \mathrm{WTI}_{t+h} \;=\; \varepsilon_j \, \theta_h^{(j)}.$$

Given a baseline real price level P_0, the corresponding price path in levels is obtained by exponentiating these deviations:

$$P_{t+h}^{(j)} \;=\; P_0 \exp\!\big(\varepsilon_j \, \theta_h^{(j)}\big).$$

This mapping is implemented in `extract_wti_irf_from_var.m`, which reads the SVAR impulse responses, cumulates the log-difference responses and returns scenario-specific

trajectories for the real WTI price. These paths are then used in Chapter 4 to construct the baseline, supply-shock and demand-shock scenarios for the stress-testing exercise.

Chapter 4

Stress Testing and Risk Engineering Application

4.1 Industrial Risk Exposure

Fuel price volatility represents one of the most significant sources of operational risk for transportation-intensive industries. Among all sectors, commercial aviation is structurally the most exposed: jet fuel typically accounts for 20–35% of operating expenses, making airlines highly sensitive to oil market disturbances. Variations in the real price of WTI translate almost immediately into changes in jet-fuel costs, impacting cash flows, budget stability and short-term liquidity. This risk is inherently systemic, as it is driven by global supply and demand forces, inventory behaviour and geopolitical tensions.

From an engineering perspective, hedging denotes a set of quantitative tools designed to reduce the variance of a firm's cost structure when exposed to volatile external inputs. The goal is not to predict prices or maximise profit, but to reduce uncertainty and stabilise operational planning. For airlines, hedging fuel costs therefore constitutes a risk engineering problem: the task is to mitigate exposure to structural shocks in oil markets in a way that aligns with operational constraints, regulatory requirements and financial limits.

4.1.1 Aviation-Specific Vulnerability

The aviation sector is uniquely exposed because its core input (jet fuel) is directly tied to crude oil markets, which exhibit strong nonlinear responses to shocks. Flow supply disruptions, global demand expansions and precautionary inventory behaviour all generate distinct price patterns, as shown in Chapter 3. Airlines cannot store large quantities of fuel nor easily substitute it, and the fleet utilisation model (high-frequency operations, seasonal variability, hub scheduling) makes cost predictability essential.

ITA Airways, like most European carriers, displays a marked seasonal pattern in flight operations, with strong peaks during the summer months and troughs in winter. This directly translates into a seasonal pattern of monthly fuel consumption. Based

on a conservative engineering analysis of flight operations, fleet utilisation and historical seasonality patterns, the annual jet-fuel consumption for 2023 is estimated at approximately 3.5 million barrels (medium scenario), with plausible bounds ranging from 3.2 to 4.0 million barrels.[1]

4.2 Scenario Construction (SVAR-Based)

Using the SVAR identification framework developed in Chapter 3, and following standard oil-market VAR practice[14, 15, 5], structural shocks can be mapped into real WTI price trajectories. The MATLAB script `stress_test_hormuz_VAR.m` produces three benchmark scenarios, saved in `stress_hormuz_VAR_results.mat`:

- `P_baseline_USD`: VAR median projection with no structural disturbance.
- `P_supply_USD`: WTI trajectory under a large negative supply shock (Hormuz-type).
- `P_demand_USD`: WTI trajectory under a large positive aggregate demand shock.

Table 4.1 summarises the implied WTI levels over the first year under each scenario.

Table 4.1: WTI price levels under baseline, supply-shock and demand-shock scenarios (first 12 months).

Month	Baseline	Supply Shock	Demand Shock
Jan	60.0	60.0	60.0
Feb	60.0	72.2	62.6
Mar	60.0	93.9	63.4
Apr	60.0	82.0	63.7
May	60.0	76.9	63.1
Jun	60.0	77.8	62.9
Jul	60.0	72.5	62.6
Aug	60.0	78.0	62.3
Sep	60.0	84.1	61.8
Oct	60.0	75.6	61.2
Nov	60.0	95.2	62.0
Dec	60.0	98.6	62.9

Note: Values rounded to one decimal place.

[1] A transparent, scenario-based reconstruction of ITA Airways' 2023 jet-fuel consumption—including operational data, fleet composition, fuel-burn benchmarks and cross-checks against comparable European carriers—is documented in Appendix C. The appendix summarises the same methodology presented in the internal technical report "Stima Conservativa del Consumo Carburante Annuale di ITA Airways (2023)", 2024.

4.2.1 From Structural Shocks to Price Paths

Let $\theta_h^{(j)}$ denote the impulse response of real WTI at horizon h to shock $j \in \{s, d, p\}$. For a shock of magnitude ε_j, the corresponding WTI path is

$$\Delta \mathrm{WTI}_{t+h}^{\mathrm{real}} = \varepsilon_j \cdot \theta_h^{(j)}.$$

The MATLAB script `extract_wti_irf_from_var.m` implements this mapping, converting structural disturbances into trajectories for the real WTI price. For the risk-engineering application, these real-price paths are interpreted as constant-(2024)-dollar WTI prices; all scenario figures are therefore reported in real USD per barrel, abstracting from residual discrepancies between deflated and nominal series. A concise description of the script structure and its role in the stress-testing pipeline is provided in Appendix C.

4.2.2 Baseline Scenario

The baseline path (`P_baseline_USD`) follows the median projection of the VAR and reflects a neutral environment without structural shocks. It captures the intrinsic persistence and autocorrelation structure of the oil market.

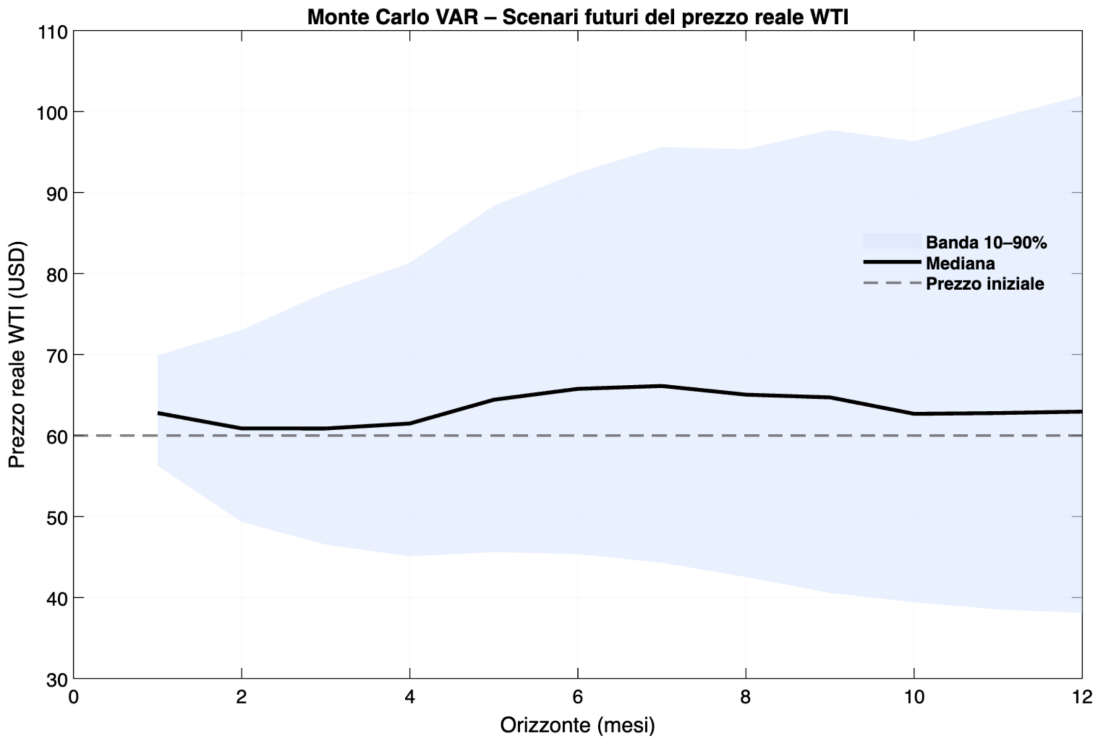

Figure 4.1: Monte Carlo VAR baseline forecast of the real WTI price. The solid line reports the median projection and the shaded area the 10–90% prediction band around the initial price level.

4.2.3 Hormuz Supply Shock Scenario

The Hormuz-type shock is modelled as a very large negative flow supply disturbance corresponding to roughly eleven standard deviations of the estimated supply shock distribution. The shock magnitude is calibrated so that the real WTI price in the stress scenario rises to slightly more than twice the baseline level after one year (an increase of about 100–110%), consistent with an extreme disruption of exports through the Strait of Hormuz [14, 5]. The scenario `P_supply_USD` exhibits:

- an immediate and pronounced jump in WTI relative to the baseline path;
- a cumulative increase in the real WTI price of around 100% at the 12-month horizon;
- gradual mean reversion over the subsequent months, with prices remaining substantially above the baseline throughout the 24-month stress-test window.

4.2.4 Demand-Driven Spike Scenario

The demand-shock scenario (`P_demand_USD`) corresponds to a two-standard-deviation aggregate demand expansion. This generates:

- a gradual increase in WTI;
- persistent effects lasting up to 18 months;
- higher long-run price levels relative to supply-driven shocks.

Demand-driven scenarios typically reflect global economic expansions, rising industrial output and increased mobility demand.

4.3 Mapping WTI to Jet-Fuel Costs

4.3.1 Pass-Through Model

The link between crude oil prices and jet fuel is approximated using the regression estimated in `estimate_pass_through_jetfuel.m` on monthly Jet Fuel USGC spot prices from the U.S. Energy Information Administration[30]. Starting from a log–log specification, the pass-through is linearised around a benchmark WTI level of 60 USD/bbl:

$$\widehat{JF}_t = \alpha_{\text{lin}} + \beta_{\text{lin}} \cdot WTI_t,$$

where JF_t denotes the Jet Fuel USGC spot price. The pass-through coefficient β_{lin} captures the proportion of crude price changes transmitted to jet fuel in a local neighbourhood of the calibration point.

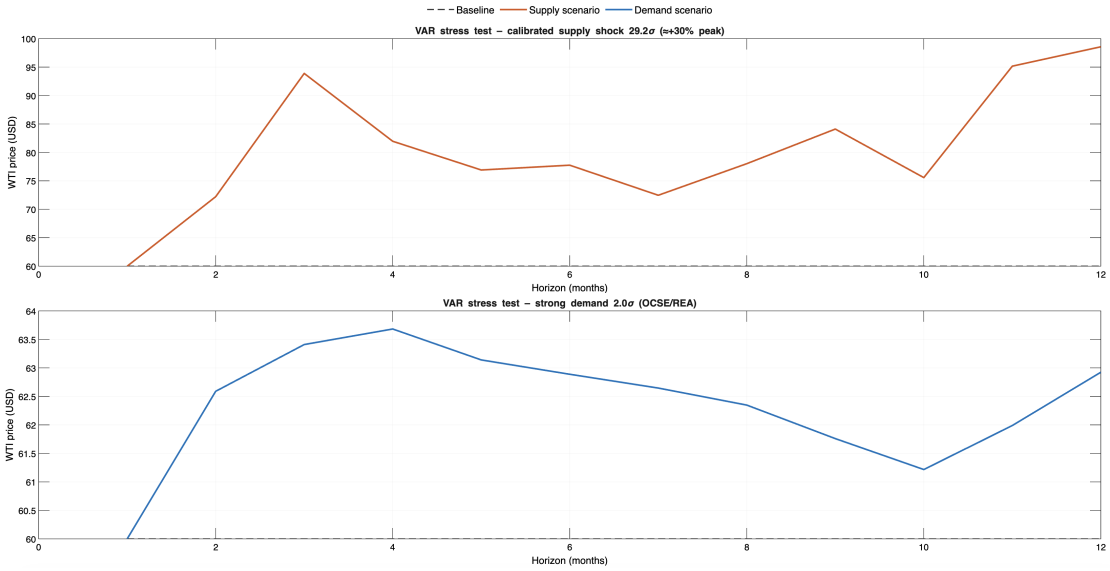

Figure 4.2: Real WTI price trajectories under baseline, supply-shock and demand-shock scenarios. The dashed line reports the baseline path, while the solid lines correspond to the calibrated Hormuz-type supply shock and the strong aggregate demand shock.

Table 4.2: Linear pass-through regression of Jet Fuel USGC prices on WTI.

Coefficient	**Estimate**
α_{lin}	-27.7001
β_{lin}	3.6532
R^2	0.790

Note: α_{lin} and β_{lin} are obtained by linearising the log–log pass-through equation at WTI = 60 USD/bbl. Standard errors are not reported because the linearised coefficients are analytically derived rather than directly estimated. The resulting relation should be interpreted as a local approximation rather than a full structural pricing model.

4.3.2 Validation

Residual diagnostics confirm:

- limited autocorrelation;
- no severe heteroscedasticity;
- a reasonable in-sample fit for a simple linear approximation.

A scatter plot of observed vs. fitted jet fuel prices is shown in Figure 4.3.

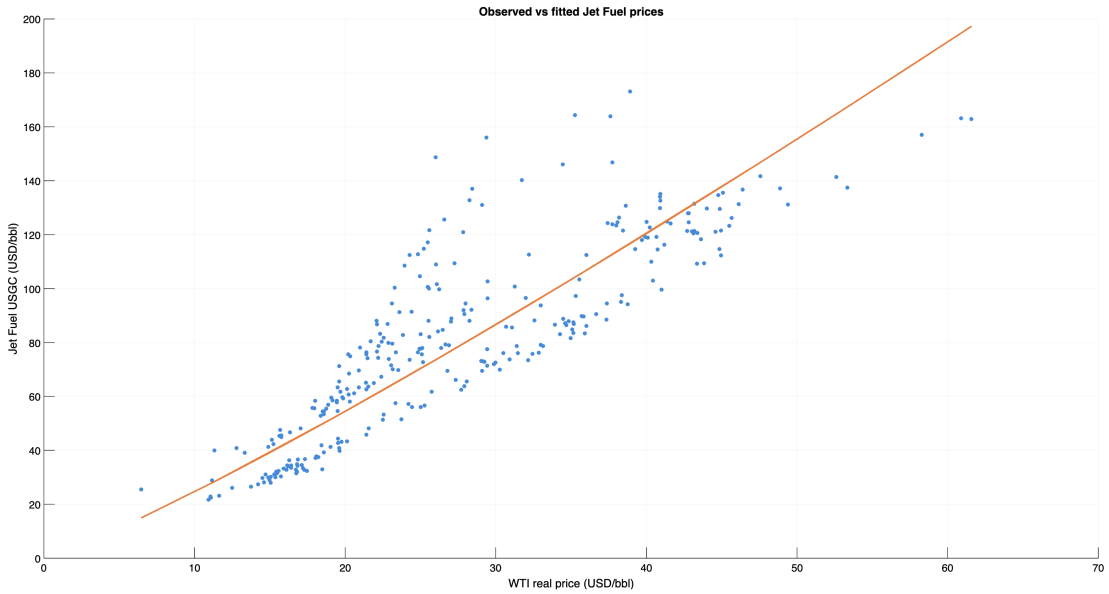

Figure 4.3: Observed vs. fitted Jet Fuel USGC prices via linear pass-through.

4.3.3 Scenario Mapping

For each WTI scenario $\mathrm{WTI}_{t+h}^{(k)}$, the corresponding jet-fuel price path is:

$$JF_{t+h}^{(k)} = \alpha_{\text{lin}} + \beta_{\text{lin}} \cdot \mathrm{WTI}_{t+h}^{(k)}.$$

These jet-fuel paths form the basis for computing monthly and annual operating costs under different environments.

4.4 Risk Scenarios

4.4.1 Monthly Fuel Consumption Allocation

Following Eurocontrol seasonal flight patterns and the technical analysis of ITA Airways' 2023 operations, annual fuel consumption (C_{annual}) is distributed across months using the following weights:

$$w = (0.06, 0.06, 0.08, 0.085, 0.09, 0.095, 0.105, 0.105, 0.09, 0.085, 0.07, 0.08),$$

which sum to 1. Monthly consumption is therefore modelled deterministically as

$$C_m = w_m \cdot C_{\text{annual}}.$$

Table 4.3 reports the full set of seasonal weights used in the stress tests.

Table 4.3: Seasonal allocation weights for monthly jet-fuel consumption.

Month	Jan	Feb	Mar	Apr	May	Jun	Jul	Aug	Sep	Oct	Nov	Dec
Weight	0.06	0.06	0.08	0.085	0.09	0.095	0.105	0.105	0.09	0.085	0.07	0.08

4.4.2 Baseline Scenario

The baseline cost is:

$$\text{Cost}_m^{\text{baseline}} = C_m \cdot JF_m^{(\text{baseline})}.$$

4.4.3 Supply-Shock Scenario

The Hormuz supply shock increases jet-fuel prices immediately and sharply:

$$\text{Cost}_m^{\text{supply}} = C_m \cdot JF_m^{(\text{supply})}.$$

4.4.4 Demand-Shock Scenario

The demand shock results in a more persistent cost increase:

$$\text{Cost}_m^{\text{demand}} = C_m \cdot JF_m^{(\text{demand})}.$$

Table 4.4: Annual fuel cost under baseline, supply-shock and demand-shock scenarios.

Scenario	**Annual Cost (USD)**	**Deviation from Baseline**	**Percent Change**
Baseline	700.00 mln	0	0%
Supply Shock	974.48 mln	274.48 mln	39.2%
Demand Shock	731.82 mln	31.82 mln	4.5%

4.5 Hedging Strategies

4.5.1 Futures Contracts

A standard futures hedge fixes the purchase price:

$$\text{Hedged Cost}_m^F = C_m \cdot F,$$

where F is the futures price. The variance of fuel cost decreases, while the expected cost may rise or fall depending on market conditions.

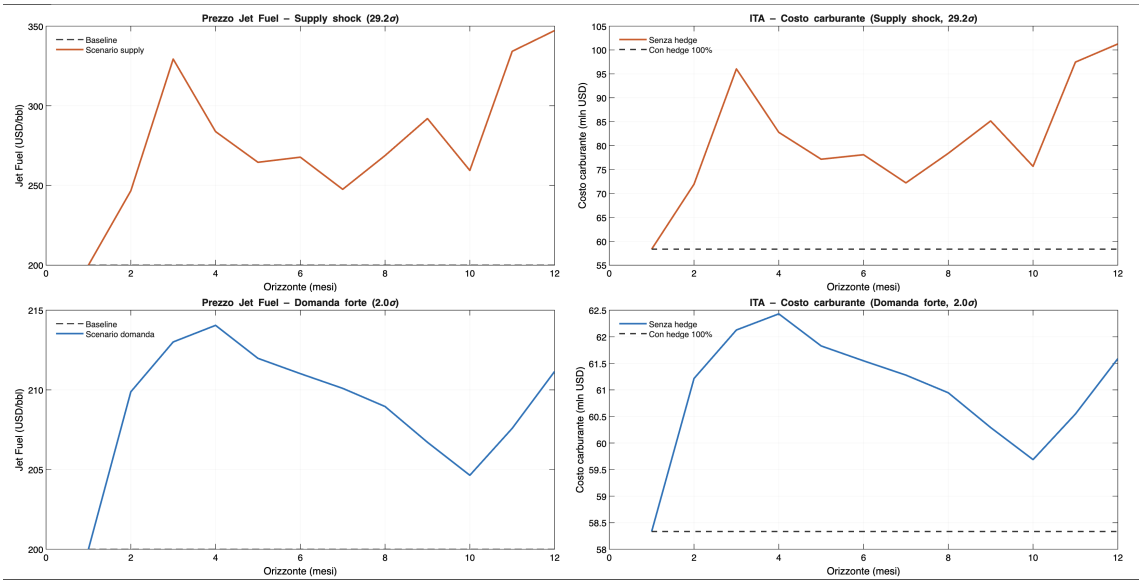

Figure 4.4: Jet fuel price and ITA Airways fuel cost under a Hormuz-type supply shock. The upper panel reports the Jet Fuel path under the calibrated supply shock (baseline vs. stress scenario); the lower panel shows the corresponding monthly fuel cost with and without a 100% linear hedge.

4.5.2 Swaps

A fixed-for-floating swap ensures:

$$\text{Hedged Cost}_m^S = C_m \cdot S_{\text{fixed}},$$

independent of jet-fuel spot prices. Swaps provide full linear protection but require credit support.

4.5.3 Collars

A zero-cost collar defines upper and lower bounds:

- floor price: $P_{\min}$ via selling a put;
- cap price: $P_{\max}$ via buying a call.

This yields asymmetric protection at zero initial cost, at the expense of giving up part of the upside if prices fall.

4.6 Impact Analysis

4.6.1 Cost Reduction

In the three benchmark scenarios, a full linear hedge transforms the fuel-cost profile from one that closely tracks spot jet-fuel prices to one that is nearly flat across months. In the

Hormuz supply-shock case, the hedge prevents the large temporary spike in fuel expenditure, keeping the annual fuel bill close to the baseline level despite the underlying price shock. In the more moderate demand-shock scenario, the hedge likewise dampens the cumulative cost increase, at the expense of foregoing potential savings in states where prices would have fallen below the locked-in level.

4.6.2 Engineering Decision Implications

Within this stylised setup, the results imply that fuel hedging:

- can stabilise operational fuel budgets in the presence of large oil-market shocks;
- reduces exposure to adverse price scenarios such as a Hormuz-type supply disruption;
- can support more reliable capacity and pricing decisions, even though these operational links are not modelled explicitly in this thesis;
- improves the robustness of medium-term financial planning under extreme but plausible stress scenarios.

Chapter 5

Conclusions

This thesis developed a comprehensive econometric and engineering framework for analysing oil market dynamics and assessing fuel price risk for aviation. The approach integrated structural macroeconomic modelling, nonlinear dependence analysis and scenario-based stress testing, culminating in an applied hedging case study for ITA Airways. The methodology combined VAR/SVAR identification, copula theory and engineering risk evaluation, with all empirical components implemented through reproducible MATLAB procedures.

5.1 Summary of Findings

The empirical results confirm the fundamental role of structural shocks in shaping oil price behaviour. Using a VAR(12) estimated on real WTI prices, U.S. crude oil production, OECD industrial activity and inventories, and identifying shocks via sign and elasticity restrictions, the analysis recovered flow supply, aggregate demand and precautionary demand disturbances consistent with the literature [14, 15, 5].

Impulse responses revealed that:

- supply shocks have strong but short-lived effects on oil prices;
- aggregate demand shocks generate persistent increases in prices and production;
- precautionary shocks produce sharp and immediate reactions, reflecting expectations of future scarcity.

The forecast error variance decomposition confirmed that medium-run price variability is dominated by demand shocks, whereas short-run volatility is closely linked to precautionary behaviour. Historical decompositions reproduced major episodes of oil price instability, including the 2003–2008 boom, the 2008 collapse and the 2014 shale-related decline.

Beyond marginal behaviour, the dependence structure of shocks was examined using copula models. Strong asymmetric tail dependence between aggregate and precautionary shocks was observed, highlighting the importance of nonlinear interactions during episodes

of heightened uncertainty. These results *motivate* the construction of stress scenarios that consider joint extreme realisations of structural shocks, even though the copula estimates are used in a primarily diagnostic rather than generative fashion.

The stress-testing module translated structural disturbances into WTI price paths using the identified impulse responses. Three benchmark scenarios were constructed: a baseline environment, a severe supply disruption reflecting a Hormuz-type event, and a demand-driven price spike. These were then mapped into jet fuel price trajectories using a simple log–log pass-through specification, locally linearised around a benchmark WTI price.

Monthly fuel costs for ITA Airways were computed by integrating these price paths with a deterministic, seasonally adjusted fuel consumption profile based on Eurocontrol traffic patterns and internal engineering estimates. The results showed that both supply and demand disturbances can generate substantial increases in monthly and annual fuel expenditure, with the Hormuz scenario producing the largest short-run impact and demand shocks generating more persistent cost pressure.

Finally, the hedging analysis evaluated three risk mitigation instruments — futures, swaps and collars — using monthly fuel consumption and scenario-based jet-fuel prices. Within the stylised three-scenario setup, all instruments flattened the fuel-cost profile relative to the unhedged case: swaps delivered the strongest smoothing of scenario-to-scenario differences, while collars provided asymmetric protection against upside price spikes at the expense of forfeiting some downside gains. These findings illustrate the potential engineering value of financial hedging as a means of stabilising operational budgets and mitigating exposure to structural oil market risk under extreme but plausible scenarios.

5.2 Implications

The results carry several implications for firms operating in fuel-intensive sectors:

- **Structural understanding matters:** distinguishing between supply, aggregate demand and precautionary shocks is critical for designing robust hedging strategies and avoiding misinterpretation of market signals.
- **Demand shocks dominate long-run price behaviour:** firms should place significant weight on macroeconomic indicators when evaluating medium-term exposure.
- **Precautionary shocks represent a key short-run risk driver:** geopolitical uncertainty and expectation-driven behaviour can produce sharp cost spikes even without physical supply losses.
- **Hedging can improve budget stability:** even in this simplified setting, more stable fuel-cost profiles can facilitate engineering decisions related to fleet planning, capacity scheduling and ticket pricing, although these operational links are not modelled explicitly in this thesis.

For policymakers and regulators, the framework demonstrates how structural modelling can support risk assessment in sectors reliant on energy commodities, and highlights the importance of transparent, timely data on production, inventories and industrial activity. These implications should, however, be interpreted in light of the modelling simplifications discussed in Section 5.3.

5.3 Limitations

The empirical analysis highlights several methodological and structural limitations that constrain the interpretation of the results and suggest caution when extrapolating beyond the scope of the thesis.

- **Reduced-form restrictions and limited explanatory power.** Although the VAR(12) successfully removes residual autocorrelation, it explains only a modest share of the variance of the real WTI price. The model captures dynamic co-movements but has limited predictive ability for the price level, as shown by the weak in-sample fit and the large role of unexplained residual shocks.
- **Heavy-tailed residuals and non-Gaussian structural shocks.** Both reduced-form residuals and structurally identified shocks exhibit pronounced excess kurtosis and asymmetric tail behaviour. Assuming approximate normality in the bootstrap-based scenario generation therefore underestimates extreme risks, despite the use of copulas to characterise dependence.
- **Parameter constancy and potential structural instability.** Rolling-window OLS results and historical episodes such as the shale revolution indicate that oil-market elasticities may vary over time. The constant-parameter VAR/SVAR framework may therefore mask regime changes in the propagation of supply, demand and precautionary shocks.
- **Linearity of the propagation mechanism.** The VAR imposes linear dynamics, whereas the copula analysis reveals strong state-dependent tail dependence, particularly between demand and precautionary shocks. Such nonlinearities are not captured by the current specification.
- **Simplified pass-through from WTI to Jet Fuel.** The pass-through model is based on a single log–log relation, locally linearised around one price point, and ignores crack-spread dynamics, refinery bottlenecks and potential asymmetries in Jet Fuel pricing. This introduces model risk when mapping WTI scenarios to fuel costs.
- **Absence of basis risk and market constraints in the hedging exercise.** The hedging application assumes a perfect hedge with no WTI–Jet Fuel basis risk, no margin requirements, no forward-curve structure and no foreign-exchange risk. These

assumptions make the results mechanically optimistic relative to realistic trading conditions.

- **Deterministic fuel consumption and limited operational detail.** Monthly Jet Fuel use follows a deterministic and highly stylised seasonal profile. Real-world airline operations exhibit substantial variability due to seasonality, load factors, aircraft mix and route structure, none of which is captured by the model; stochastic volume risk is therefore ignored.

- **Reduced-form Monte Carlo simulation.** Scenario generation relies on bootstrap sampling of VAR residuals, which preserves reduced-form dynamics but not the structural dependence patterns among shocks. As a result, structural tail dependence may be only partially reflected in simulated extremes.

These limitations do not undermine the qualitative insights of the analysis but restrict the generality of the quantitative results and motivate the extensions discussed in the following section.

5.4 Future Research Directions

The limitations discussed above naturally point to several directions for future research aimed at improving the statistical realism, structural interpretability and practical relevance of oil-market risk assessment.

- **Time-varying parameter SVARs with stochastic volatility.** The evidence of structural instability and evolving elasticities suggests moving toward TVP-SVAR or Bayesian stochastic-volatility frameworks, allowing the propagation of supply, demand and precautionary shocks to drift across regimes such as the shale revolution or crisis periods.

- **Volatility modelling with higher-frequency data.** Given the heavy-tailed residuals and volatility clustering, future work could estimate GARCH-type or stochastic-volatility models using weekly or daily data, integrating them either as stand-alone components or as volatility inputs to a multivariate model.

- **Nonlinear and regime-dependent VAR structures.** The tail dependence detected between demand and precautionary shocks motivates nonlinear specifications: threshold VARs, Markov-switching VARs or smooth-transition VARs capable of capturing state-dependent propagation under extreme market conditions.

- **Hybrid deep-learning forecasting models.** Since the VAR explains only a limited share of price-level variability, deep-learning sequence models such as LSTM or transformer architectures could complement the structural model. A hybrid

pipeline—GARCH/SV for volatility, LSTM for nonlinear interactions, SVAR for structural interpretation—may yield richer scenario generation.

- **Dynamic and higher-dimensional copula models.** Extending the copula analysis to dynamic copulas or vine copulas would allow dependence among structural shocks to evolve over time, strengthening the realism of structural scenario simulation and tail-risk quantification.

- **More realistic pass-through and basis-risk modelling.** Future work could model crack-spread dynamics, refinery capacity constraints and Jet Fuel–WTI basis risk explicitly, replacing the current linear pass-through with a structural or semi-parametric pricing relation.

- **Stochastic and operationally detailed fuel-consumption modelling.** Incorporating route-level data, aircraft utilisation, seasonal load factors and stochastic volume uncertainty would provide a more granular mapping from oil-market shocks to airline operating costs.

- **Advanced hedging optimisation under market constraints.** A rigorous extension would integrate FX risk, margin requirements, forward-curve structure, liquidity constraints and partial-hedge strategies within a stochastic programming or risk-budgeting framework.

Overall, these extensions would allow future research to bridge the gap between structural macro–oil modelling and practical risk engineering, especially in applications involving extreme-event stress testing and airline fuel-cost management.

5.5 Final Remarks

This thesis demonstrates that combining structural econometric modelling with engineering-based risk analysis offers a useful framework for understanding and mitigating fuel price exposure. By linking structural shocks, nonlinear dependence patterns and hedging instruments within an integrated stress-testing architecture, the study provides actionable insights for both academic research and industrial decision-making. The methodology is general and can be extended to other energy-intensive sectors, supporting a broader understanding of commodity price risk in complex operational environments.

Overall, the thesis advances the structural analysis of oil-market dynamics and illustrates how econometric identification, basic tail-risk considerations and engineering-driven hedging strategies can be integrated into a coherent, albeit stylised, framework for scenario-based risk assessment in fuel-intensive industries.

Bibliography

[1] Soren T. Anderson, Ryan Kellogg, and Stephen W. Salant. "Hotelling Under Pressure". In: *Journal of Political Economy* 126.3 (2018), pp. 984–1026. DOI: 10.1086/697203.

[2] Jushan Bai and Pierre Perron. "Computation and Analysis of Multiple Structural Change Models". In: *Journal of Applied Econometrics* 18.1 (2003), pp. 1–22. DOI: 10.1002/jae.659.

[3] Robert B. Barsky and Lutz Kilian. "Do We Really Know that Oil Caused the Great Stagflation? A Monetary Alternative". In: *NBER Macroeconomics Annual* 16 (2002), pp. 137–183. DOI: 10.1086/ma.16.3585277.

[4] Robert B. Barsky and Lutz Kilian. "Oil and the Macroeconomy since the 1970s". In: *Journal of Economic Perspectives* 18.4 (2004), pp. 115–134. DOI: 10.1257/0895330042632708.

[5] Christiane Baumeister and James D. Hamilton. "Structural Interpretation of Vector Autoregressions with Incomplete Identification: Revisiting the Role of Oil Supply and Demand Shocks". In: *American Economic Review* 109.5 (2019), pp. 1873–1910. DOI: 10.1257/aer.20151569.

[6] Trevor S. Breusch and Adrian R. Pagan. "A Simple Test for Heteroscedasticity and Random Coefficient Variation". In: *Econometrica* 47.5 (1979), pp. 1287–1294. DOI: 10.2307/1911963.

[7] R. L. Brown, J. Durbin, and J. M. Evans. "Techniques for Testing the Constancy of Regression Relationships over Time". In: *Journal of the Royal Statistical Society, Series B (Methodological)* 37.2 (1975), pp. 149–163. DOI: 10.1111/j.2517-6161.1975.tb01532.x.

[8] Salvatore Carollo. *Once Upon a Time There Was the Price of Oil*. Chichester: Wiley, 2010. ISBN: 9781119990312.

[9] Federal Reserve Bank of Dallas. *Index of Global Real Economic Activity (IGREA)*. Dallas Fed Globalization Institute. Monthly index as per Kilian (2009, 2019), retrieved 2025-11-27. URL: https://fred.stlouisfed.org/series/IGREA.

[10] Finnair Plc. *Annual Report 2022*. Finnair Plc, 2023. URL: https://investors.finnair.com/en/reports-and-presentations (visited on 12/01/2025).

[11] International Air Transport Association (IATA). *Fuel Efficiency in Aviation: Why It Matters More Than Ever*. IATA Knowledge Hub. Accessed: 2025-11-24. 2024. URL: https://www.iata.org/en/publications/newsletters/iata-knowledge-hub/fuel-efficiency-in-aviation-why-it-matters-more-than-ever/.

[12] Carlos M. Jarque and Anil K. Bera. "A Test for Normality of Observations and Regression Residuals". In: *International Statistical Review* 55.2 (1987), pp. 163–172. DOI: 10.2307/1403192.

[13] Lutz Kilian. "Measuring Global Real Economic Activity: Do Recent Critiques Hold Up to Scrutiny?" In: *Economics Letters* 178 (2019), pp. 106–110. DOI: 10.1016/j.econlet.2019.03.001.

[14] Lutz Kilian. "Not All Oil Price Shocks Are Alike: Disentangling Demand and Supply Shocks in the Crude Oil Market". In: *American Economic Review* 99.3 (2009), pp. 1053–1069. DOI: 10.1257/aer.99.3.1053.

[15] Lutz Kilian and Daniel P. Murphy. "The Role of Inventories and Speculative Trading in the Global Market for Crude Oil". In: *Journal of Applied Econometrics* 29.3 (2014), pp. 454–478. DOI: 10.1002/jae.2322.

[16] Lutz Kilian and Xiaoqing Zhou. "Modeling Fluctuations in the Global Demand for Commodities". In: *Journal of International Money and Finance* 88 (2018), pp. 54–78. DOI: 10.1016/j.jimonfin.2018.07.001.

[17] Lutz Kilian and Xiaoqing Zhou. *The Econometrics of Oil Market VAR Models*. Working Paper 2002. Federal Reserve Bank of Dallas, 2020. URL: https://www.dallasfed.org/research/papers/2020/wp2002.

[18] Greta M. Ljung and George E. P. Box. "On a Measure of Lack of Fit in Time Series Models". In: *Biometrika* 65.2 (1978), pp. 297–303. DOI: 10.1093/biomet/65.2.297.

[19] Helmut Lütkepohl. *New Introduction to Multiple Time Series Analysis*. Berlin Heidelberg: Springer, 2005. ISBN: 978-3-540-26239-8.

[20] Frank J. Massey. "The Kolmogorov-Smirnov Test for Goodness of Fit". In: *Journal of the American Statistical Association* 46.253 (1951), pp. 68–78. DOI: 10.1080/01621459.1951.10500769.

[21] Roger B. Nelsen. *An Introduction to Copulas*. 2nd. New York: Springer, 2006. DOI: 10.1007/0-387-28678-0.

[22] Andrew J. Patton. "A Review of Copula Models for Economic Time Series". In: *Journal of Multivariate Analysis* 110 (2012), pp. 4–18. DOI: 10.1016/j.jmva.2012.02.021.

[23] Polish Aviation Group. *Sustainable Growth: Decarbonisation Strategy 2030*. Overview of LOT Polish Airlines' fuel-efficiency and decarbonisation targets. 2020. URL: https://pgl.pl/en/sustainable-growth/ (visited on 12/01/2025).

[24] Juan F. Rubio-Ramirez, Daniel F. Waggoner, and Tao Zha. "Structural Vector Autoregressions: Theory of Identification and Algorithms for Inference". In: *Review of Economic Studies* 77.2 (2010), pp. 665–696. DOI: 10.1111/j.1467-937X.2009.00578.x.

[25] Christopher A. Sims. "Macroeconomics and Reality". In: *Econometrica* 48.1 (1980), pp. 1–48. DOI: 10.2307/1912017.

[26] Michael Sockin and Wei Xiong. "Informational Frictions and Commodity Markets". In: *Journal of Finance* 70.5 (2015), pp. 2063–2098. DOI: 10.1111/jofi.12298.

[27] TAP Air Portugal. *Relatório de Sustentabilidade 2022*. Transportes Aéreos Portugueses S.A., 2023. URL: https://www.tapairportugal.com/pt/sobre-nos/relatorios-anuais (visited on 12/01/2025).

[28] U.S. Bureau of Labor Statistics. *Consumer Price Index for All Urban Consumers: All Items*. FRED, Federal Reserve Bank of St. Louis. Series CPIAUCSL, retrieved 2025-11-27. URL: https://fred.stlouisfed.org/series/CPIAUCSL.

[29] U.S. Energy Information Administration. *Crude Oil Prices: West Texas Intermediate (WTI) – Cushing, Oklahoma*. FRED, Federal Reserve Bank of St. Louis. Series MCOILWTICO, retrieved 2025-11-27. URL: https://fred.stlouisfed.org/series/MCOILWTICO.

[30] U.S. Energy Information Administration. *Kerosene-Type Jet Fuel Spot Price, U.S. Gulf Coast*. EIA Petroleum Other Liquids. Dollars per gallon, monthly average, retrieved 2025-11-27. URL: https://www.eia.gov/dnav/pet/hist/LeafHandler.ashx?n=PET%5C&s=EER_EPJK_PF4_RGC_DPG%5C&f=M.

[31] U.S. Energy Information Administration. *USA Total Crude Oil and Petroleum Products Ending Stocks*. International Energy Database (EIA). Monthly data, retrieved 2025-11-27. URL: https://www.eia.gov/international/data/petroleum-and-other-liquids.

[32] U.S. Energy Information Administration. *World Crude Oil Production*. International Energy Statistics (EIA). Monthly, million barrels per day, retrieved 2025-11-27. URL: https://www.eia.gov/international/data/world/petroleum-and-other-liquids/production.

Appendix A

Data Construction and Pre-VAR Diagnostics

A.1 Data Sources, Frequency Alignment and Storage

The empirical analysis relies on monthly data spanning 1990–2024 for four key variables: global crude oil production, OECD real activity (aggregate industrial index), petroleum inventories and the real WTI price. Raw series are gathered from the sources listed in Table 2.1 in Chapter 2 and then harmonised to a common monthly calendar.

All series are first converted to end-of-month observations and aligned on a shared time index. When a series is released at a different frequency or with occasional missing values, the following conventions are applied:

- quarterly or higher-frequency observations are aggregated or averaged to the monthly frequency, preserving the timing conventions of the original release;
- isolated missing entries are linearly interpolated only when this is necessary to avoid spurious gaps within otherwise continuous stretches of data; no series is forward- or backward-filled over extended periods;
- outlier values clearly attributable to data errors are replaced by the median of a narrow neighbourhood, with all adjustments documented in the `build_oil_dataset.m` script.

After alignment, three data structures are created and stored in `clean_data.mat`:

- `All`: timetable of raw levels or log-levels (real WTI price, crude oil production, OECD activity index, petroleum inventories);
- `All_d`: timetable of stationary transformations (first differences or $\Delta \log$ transforms), subsequently standardised to zero mean and unit variance;

- `ALL_VAR`: numeric matrix used as input for the VAR estimation, with columns ordered as Production, OECD, WTI and Inventories and rows corresponding to common monthly dates.

The OECD activity index is chosen as the global demand proxy because, within the sample, it displays a more stable dynamic relationship with the real WTI price than the IGREA index, while avoiding some of the measurement revisions associated with shipping-based indicators [14, 13].

A.2 Transformations and Stationarity Checks

The construction of `All_d` follows the standard practice of rendering the series approximately covariance-stationary before specifying a VAR.

- Crude oil production, the real WTI price and inventories are transformed using $\Delta \log$ differences, which correspond approximately to monthly percentage changes.
- The OECD activity index is decomposed into a low-frequency trend and a cyclical component; the latter (denoted `OECD_cycle`) is used in the VAR to capture global business-cycle fluctuations around the long-run level.
- Each stationary transformation is then standardised to zero mean and unit variance, so that the corresponding VAR coefficients and impulse responses are expressed in comparable units.

Augmented Dickey–Fuller (ADF) tests are applied both to the original levels and to the transformed series. In levels, the null of a unit root cannot be rejected for any of the four variables at conventional significance levels, consistent with the large literature documenting non-stationarity in oil prices, production, inventories and activity indicators. In contrast, all transformed series in `All_d` exhibit ADF p-values well below the 5% threshold, supporting the use of the VAR in differences and cycle form.

To complement formal tests, pre-VAR diagnostics include visual inspection of time-series plots, autocorrelation functions and ADF p-value charts for each variable. These confirm that the transformed series fluctuate around a stable mean with no obvious residual trends or explosive behaviour.

A.3 Baseline Static Regression and Diagnostics

Before moving to a multivariate dynamic specification, a benchmark static regression is estimated to assess whether contemporaneous linear relationships between the transformed fundamentals and the oil price can explain a meaningful share of its variation. The regression is specified as:

$$WTI_t^{DL} = \beta_0 + \beta_1 \,\text{Production}_t^{DL} + \beta_2 \,\text{OECD}_t^{DL} + \beta_3 \,\text{Inventories}_t^{DL} + u_t,$$

where the superscript DL denotes Δ log-transformed variables. Although this formulation already removes deterministic trends and stabilises variances, the model attains only a very modest adjusted R^2 (approximately 0.11), indicating that contemporaneous fundamentals have limited explanatory power for the monthly change in the real WTI price.

Residual diagnostics for this OLS specification reveal:

- strong serial correlation, as indicated by Ljung–Box statistics with p-values well below 1%;
- pronounced heteroskedasticity according to Breusch–Pagan tests ($p \approx 0.0000$);
- clear deviations from normality, with heavy tails relative to the Gaussian benchmark.

Rolling-window estimates of the coefficients further display substantial instability across subsamples, especially around major structural episodes such as the early-2000s boom and the post-2010 shale expansion. Together, these diagnostics suggest that the static OLS framework is inadequate for capturing the dynamics of oil prices and motivates the move to a multivariate, dynamic VAR/SVAR approach.

A.4 Distributional Properties of OLS Residuals

The residuals u_t from the baseline regression provide an initial window on the distributional features of unexplained oil-price movements. Empirical density plots, histograms and normal Q–Q plots point to marked departures from Gaussianity:

- the residual distribution exhibits mild negative skewness, reflecting occasional large downward adjustments in the real WTI price;
- excess kurtosis indicates a leptokurtic shape, with more probability mass in the centre and in the tails than a normal distribution;
- extreme observations are clustered around well-known market events (price collapses and sharp spikes), rather than being isolated outliers.

These features justify the use of bootstrap methods in subsequent stages (impulse-response confidence bands, scenario generation) and provide preliminary evidence that non-Gaussian shocks may be structurally relevant in the oil market. In particular, the heavy tails and asymmetric behaviour of u_t are consistent with the presence of large, infrequent structural disturbances, which are modelled explicitly in the SVAR framework developed in Chapters 3 and 4.

Appendix B

VAR–SVAR Framework and Shock Dependence

B.1 Reduced-Form VAR Specification

The reduced-form VAR is estimated on the vector of stationary transformations

$$y_t = \begin{bmatrix} \text{Production}_t^{DL} \\ \text{OECD\_cycle}_t \\ \text{WTI}_t^{DL} \\ \text{Inventories}_t^{DL} \end{bmatrix},$$

where DL denotes $\Delta \log$ transformations and `OECD_cycle` is the cyclical component of the OECD activity index. Each component of y_t is standardised to zero mean and unit variance before estimation, so that the resulting coefficients and shocks are directly comparable across variables.

The VAR(p) in companion form is

$$y_t = A_1 y_{t-1} + \cdots + A_p y_{t-p} + u_t, \quad u_t \sim (0, \Sigma_u),$$

with the ordering

$$\text{(Production, OECD, WTI, Inventories)}.$$

Lag-length selection is performed over $p = 1, \ldots, 15$ using a combination of information criteria, residual autocorrelation tests and stability checks on the companion matrix eigenvalues. All criteria point to relatively long dynamics, and residual portmanteau tests reject low-order specifications. A lag length of $p = 12$ is ultimately selected as a compromise between capturing the long adjustment horizons typical of global oil markets and preserving a reasonable number of effective observations.

The script `var_main.m` implements this procedure and stores the estimated coefficient matrices and residuals, which serve as the basis for the subsequent structural analysis.

B.2 Benchmark Cholesky Identification

As a preliminary step, a recursive (Cholesky) identification is applied to the reduced-form residuals u_t. The covariance matrix Σ_u is factorised as $\Sigma_u = PP'$ and the orthogonalised innovations $\tilde{\varepsilon}_t = P^{-1}u_t$ are interpreted as shocks ordered according to (Production, OECD, WTI, Inventories).

The associated Cholesky impulse responses provide a diagnostic benchmark:

- aggregate-demand disturbances (innovations to OECD activity) account for a large fraction of the forecast error variance of the real WTI price at medium horizons;
- shocks to crude oil production generate modest and short-lived price responses;
- inventory innovations produce noisy and moderately persistent effects.

These patterns are broadly in line with the structural interpretation proposed in the literature, but the recursive scheme is inherently sensitive to the chosen ordering and cannot be given a fully structural meaning. It is therefore used only as a starting point for assessing the plausibility of the data and guiding the design of sign restrictions.

B.3 Structural Identification via Sign Restrictions

Structural shocks are identified using sign restrictions in the spirit of Kilian and Murphy [15]. Let

$$u_t = B\varepsilon_t,$$

where B is the contemporaneous impact matrix and $\varepsilon_t = (\varepsilon_t^s, \varepsilon_t^d, \varepsilon_t^p, \varepsilon_t^{\text{other}})'$ collects the structural disturbances: flow supply (s), aggregate demand (d), precautionary (or storage) demand (p) and a residual "other" shock.

Starting from a particular decomposition B_0 such that $\Sigma_u = B_0 B_0'$, a large number of candidate impact matrices are generated via random orthogonal rotations Q:

$$B = B_0 Q, \qquad Q'Q = I.$$

For each candidate B, the corresponding impulse responses are computed and retained only if they satisfy the following sign restrictions over a short horizon (typically $h = 1, \ldots, 12$):

- **Flow supply shock** (ε^s): Production $\downarrow$, WTI $\uparrow$;
- **Aggregate-demand shock** (ε^d): OECD $\uparrow$, Production $\uparrow$, WTI $\uparrow$;
- **Precautionary/storage shock** (ε^p): WTI $\uparrow$, Inventories $\uparrow$.

Out of 100,000 random orthogonal rotations drawn in `svar_sign_restrictions.m`, only a handful (six) satisfy all the restrictions simultaneously. This low acceptance rate

indicates that the restrictions are informative and tightly pin down the economically relevant decomposition of shocks. All structural results reported in the main text are computed as medians across the accepted draws, with percentile bands used to capture the remaining identification uncertainty.

B.4 Structural Impulse Responses and Variance Decomposition

The structural impulse responses obtained from the accepted B matrices reveal a clear pattern:

- aggregate-demand shocks produce the strongest and most persistent increases in the real WTI price, together with sustained increases in production and economic activity;
- flow supply shocks generate moderate but economically meaningful price responses that decay relatively quickly, with production falling on impact and gradually recovering;
- precautionary shocks display hump-shaped short-run dynamics in the oil price and inventories, consistent with temporary inventory accumulation driven by expectations of future scarcity.

The corresponding forecast error variance decomposition (reported in Chapter 3) shows that demand shocks dominate the medium-run variance of the real WTI price, while precautionary shocks contribute disproportionately to very short-run volatility. Supply shocks play a more limited but non-negligible role.

B.5 Marginal Distributions of Structural Shocks

To analyse the distributional properties of structural shocks, the accepted draws of $(\varepsilon_t^s, \varepsilon_t^d, \varepsilon_t^p)$ are assembled and standardised. The script `fit_marginal_shocks.m` then fits several parametric families to each marginal by maximum likelihood, including Gaussian, Logistic and Student-t distributions.

Across all three shocks, Gaussian and Logistic specifications systematically underestimate the empirical tail thickness. Student-t marginals with finite degrees of freedom provide a markedly better fit, capturing both the leptokurtosis and, for demand and precautionary shocks, pronounced skewness. These findings reinforce the evidence from pre-VAR diagnostics that heavy-tailed shocks are a salient feature of oil-market dynamics and motivate their use in the copula-based dependence analysis.

B.6 Copula-Based Dependence

Dependence among structural shocks is studied using bivariate copulas fitted to pairs $(\varepsilon_t^i, \varepsilon_t^j)$ after transforming each marginal to the unit interval via the fitted Student-t distributions. The `copula_fit_shocks.m` script compares several families—Gaussian, Student-t, Clayton, Gumbel and Frank—using pseudo-likelihood criteria.

The main qualitative findings are:

- a Student-t copula with low degrees of freedom ($\nu \approx 3.4$) best describes the joint behaviour of aggregate-demand and precautionary shocks, implying strong upper-tail dependence: large positive demand shocks tend to coincide with large positive precautionary shocks;
- dependence between flow supply and precautionary shocks is weaker and more symmetric, with a Frank copula providing the best fit;
- dependence between flow supply and aggregate-demand shocks is moderate and close to elliptical, and can be captured reasonably well by either a Gaussian or a mild Student-t copula.

These patterns suggest that episodes of strong global demand are often accompanied by inventory-accumulation behaviour and expectation-driven pressures, thereby amplifying oil price spikes. The copula analysis is used here in a purely *diagnostic* fashion: it characterises how shocks co-move in the historical sample and motivates the construction of joint stress scenarios, but it does not yet feed directly into the scenario generator of Chapter 4.

B.7 Conditional Tail Probabilities

Using the fitted copulas, the script `copula_prob_cond_shocks.m` computes conditional probabilities of joint extreme events. In particular, interest centres on the probability that one shock exceeds a high quantile conditional on another shock being large:

- the probability that the precautionary shock exceeds its 90th percentile given that the aggregate-demand shock is above its 90th percentile is found to be in the range of 35–45%, consistent with strong upper-tail dependence between the two;
- in contrast, the probability that the precautionary shock is extreme conditional on a large negative flow supply shock remains below 10%, reflecting the weaker and more symmetric dependence between supply and precautionary disturbances.

These conditional tail probabilities highlight that extreme demand episodes are the most likely environment in which large precautionary shocks materialise, providing a structural rationale for focusing stress scenarios on joint demand and precautionary disturbances. A full integration of copula-based simulation into the scenario generator is left to future research and outlined in Chapter 5.

B.8 Additional VAR Diagnostic: Residual Distribution

Figure B.1 reports the histogram of standardised residuals for the WTI equation in the VAR(12), overlaid with a standard normal density. The heavy tails and mild asymmetry relative to the Gaussian benchmark are consistent with the evidence discussed in Appendix A and motivate the use of bootstrap methods and heavy–tailed marginals in the copula analysis.

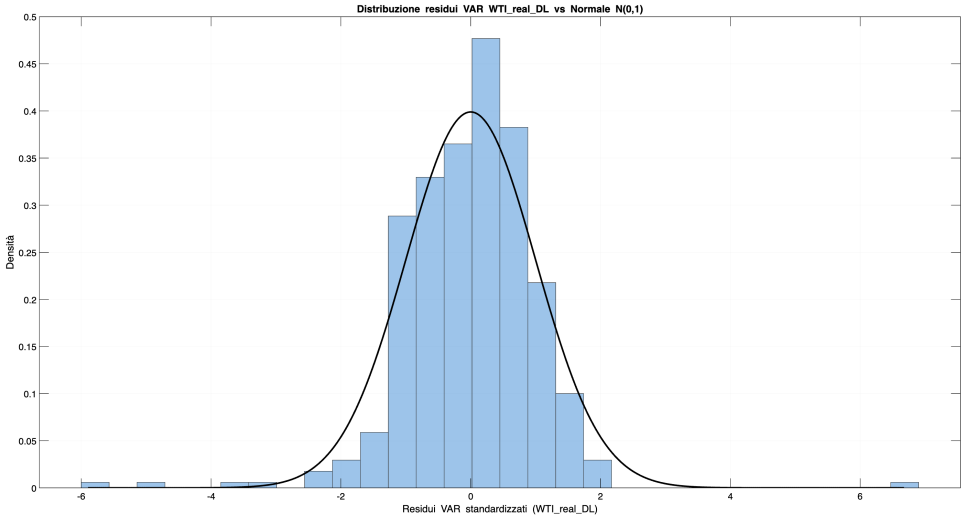

Figure B.1: Standardised residuals of the WTI equation in the VAR(12) versus a standard normal density.

Appendix C

ITA Airways Fuel Demand Estimation

C.1 Purpose and Context

The hedging simulations developed in the main analysis require a realistic estimate of ITA Airways' annual jet-fuel consumption. Since the airline does not publicly disclose its physical fuel-use figures, the value must be inferred indirectly using operational data, fleet characteristics and standard aviation fuel-burn benchmarks.

This appendix documents the procedure followed to obtain a transparent and conservative estimate suitable for modelling fuel-price exposure. The goal is not to reconstruct exact accounting values, but to generate a consistent operational estimate applicable to the stress-testing and hedging framework.

C.2 Underlying Operational Data

The estimation relies on publicly available information for the year 2023:

- **Scheduled flights:** approximately 124,000 across domestic, intra-European and long-haul routes.
- **Passengers:** roughly 15 million carried, with an average load factor of about 79%.
- **Fleet:** 96 Airbus aircraft, including a growing share of new-generation aircraft (A220, A320neo, A330neo, A350).
- **Network structure:** operations distributed across:
  - Domestic and short-haul European routes (< 2.5 hours),
  - Medium-haul routes (2.5–5 hours),
  - Long-haul intercontinental routes (North America, South America, Middle East, India).

C.3 Fuel-Burn Benchmarks and Adjustments

Average per-flight fuel-burn benchmarks are sourced from industry technical reports and aircraft flight-performance documentation:

- Narrow-body aircraft (short/medium haul): 2.5–3.0 tonnes/flight.
- Wide-body aircraft (long haul): 40–55 tonnes/flight.

To account for real-world operational inefficiencies (congestion, taxi time, step climbs, airspace restrictions, payload variability), a +10% adjustment is applied.

The following conversion factor is used throughout:

$$1 \text{ tonne Jet-A1} \approx 7.9 \text{ barrels.}$$

C.4 Scenario-Based Estimation Method

Due to incomplete route-level public data, fuel consumption is modelled using a scenario-based aggregation:

$$Q_{\text{jet}} = N_{\text{SR}}\, q_{\text{SR}} + N_{\text{LH}}\, q_{\text{LH}},$$

where $N_{\text{SR}}, N_{\text{LH}}$ denote the number of short-/medium-haul and long-haul flights, and $q_{\text{SR}}, q_{\text{LH}}$ represent corresponding fuel-burn averages.

Instead of fixing values at a granular level, three internally consistent scenarios are constructed to capture uncertainty in:

- mix of long-haul versus short-/medium-haul flying,
- share of new-generation versus legacy aircraft,
- seasonal variation and utilisation rates,
- operational efficiency and route constraints.

C.4.1 Scenario Results

Table C.1: Estimated 2023 fuel consumption under alternative scenarios.

Scenario	Fuel (Mt)	Fuel (million barrels)	Notes
Minimum	≈ 0.40	≈ 3.2	High efficiency, shorter route structure and high share of new-generation aircraft.
Central	0.44–0.45	3.5–3.6	Reflects observed 2023 utilisation, fleet composition and route distribution.
Maximum	0.49–0.50	3.9–4.0	Higher long-haul share, lower efficiency and greater legacy aircraft operation.

C.5 Cross-Validation Against Comparable Airlines

To validate plausibility, the estimated range is benchmarked against *approximate 2022 jet-fuel use reconstructed from public environmental and sustainability disclosures* of airlines with similar fleet size and network structure:[1]

- Finnair (2022): ~ 0.79 Mt,
- TAP Air Portugal (2022): ~ 0.58 Mt,
- LOT Polish Airlines (2022): ~ 0.45 Mt.

Given ITA's long-haul expansion in 2023 and the partial transition toward newer aircraft, the estimated 0.44–0.50 Mt range is consistent with these comparators.

C.6 Financial Consistency Check

To ensure internal consistency with typical airline economics, fuel cost implications are evaluated using a reference wholesale price range:

$$\$700 \leq P_{\text{Jet Fuel}} \leq \$1,050 \text{ per tonne.}$$

This implies:

$$280 \text{ M€} \leq \text{Annual Fuel Cost} \leq 525 \text{ M€},$$

which aligns with the 20–35% cost share commonly observed among European network carriers.

[1] Approximate values obtained by combining CO_2-emissions and fuel-efficiency indicators reported in the 2022 sustainability/annual reports of Finnair, TAP Air Portugal and LOT Polish Airlines; see, for example, Finnair Plc [10], TAP Air Portugal [27], and Polish Aviation Group [23].

C.7 Final Value Adopted in the Model

For the simulations, a single representative value is required. Based on scenario inference and validation tests, the following value is adopted:

$$Q_{\text{jet, used}} = 3.5 \times 10^6 \text{ barrels/year}.$$

This quantity provides a conservative but realistic approximation of ITA Airways' annual exposure to jet-fuel price risk.